Absence of Higher-Order Corrections in the Anomalous Axial-Vector Divergence Equation

STEPHEN L. ADLER AND WILLIAM A. BARDEEN*
Institute for Advanced Study, Princeton, New Jersey 08540
(Received 24 February 1969)

We consider two simple field-theoretic models, (a) spinor electrodynamics and (b) the σ model with the Polkinghorne axial-vector current, and show in each case that the axial-vector current satisfies a simple anomalous divergence equation exactly to all orders of perturbation theory. We check our general argument by an explicit calculation to second order in radiative corrections. The general argument is made tractable by introducing a cutoff, but to check the validity of this artifice, the second-order calculation is carried out entirely in terms of renormalized vertex and propagator functions, in which no cutoff appears.

I. INTRODUCTION

IT has recently been shown[1,2] that the axial-vector current in spinor electrodynamics does not satisfy the usual divergence equation

$$\partial^\mu j_\mu{}^5(x) = 2im_0 j^5(x),$$
$$j_\mu{}^5(x) = \bar\psi(x)\gamma_\mu\gamma_5\psi(x), \quad j^5(x) = \bar\psi(x)\gamma_5\psi(x), \tag{1}$$

expected from naive use of the equations of motion, but rather obeys the equation

$$\partial^\mu j_\mu{}^5(x) = 2im_0 j^5(x) + (\alpha_0/4\pi)F^{\xi\sigma}(x)F^{\tau\rho}(x)\epsilon_{\xi\sigma\tau\rho}, \tag{2}$$

with $F^{\xi\sigma}$ the electromagnetic field strength tensor. Similarly, it was shown that in a simple version of the Gell-Mann–Lévy σ model[3] coupled to the electromagnetic field, the axial-vector current does not satisfy the usual PCAC (partially conserved axial-vector current) equation

$$\partial^\mu j_\mu{}^5(x) = -(\mu_1{}^2/g_0)\pi(x),$$
$$j_\mu{}^5(x) = \bar\psi(x)\tfrac{1}{2}\gamma_\mu\gamma_5\psi(x) + \sigma(x)\partial_\mu\pi(x) - \pi(x)\partial_\mu\sigma(x) + g_0{}^{-1}\partial_\mu\pi(x), \tag{3}$$

but instead obeys the modified PCAC condition

$$\partial^\mu j_\mu{}^5(x) = -(\mu_1{}^2/g_0)\pi(x) + \tfrac{1}{2}(\alpha_0/4\pi)F^{\xi\sigma}(x)F^{\tau\rho}(x)\epsilon_{\xi\sigma\tau\rho}. \tag{4}$$

In both theories, the extra term in Eqs. (2) and (4) arises from the presence of the axial-vector triangle diagram shown in Fig. 1. This diagram has an anomalous property; when it is defined to be gauge-invariant with respect to its vector indices, it does not satisfy the usual axial-vector Ward identity.

An essential conclusion[4] of I was that Eqs. (2) and (4) are exact. In other words, the anomalous term $F^{\xi\sigma}F^{\tau\rho}\epsilon_{\xi\sigma\tau\rho}$ does not receive additional contributions from radiative corrections to triangles, such as shown in Fig. 2 (the wavy line denotes either a photon or a meson). This conclusion follows naively from the observation that radiative corrections to the basic triangle involve axial-vector loops (such as the five-vertex loop shown in Fig. 2) which, unlike the lowest-order axial-vector triangle, *do* satisfy the usual axial-vector Ward identity. The purpose of the present paper is to support this naive reasoning with more detailed calculations, and in particular, to show that the fact that radiative corrections to triangles involve the usual renormalizable infinities causes no trouble.

The plan of the paper is as follows. In Sec. II we consider the two models discussed in I—spinor electrodynamics and the σ model—and develop a general argument which shows that Eqs. (2) and (4) are exact. In Sec. III we give an *explicit calculation* of the second-order radiative corrections to the triangle. We find, in agreement with our general arguments, that when all of the second-order radiative corrections are summed, their contributions to the $F^{\xi\sigma}F^{\tau\rho}\epsilon_{\xi\sigma\tau\rho}$ term exactly cancel. In Sec. IV we briefly summarize our results and compare them with the conclusions reached recently by Jackiw and Johnson.[2]

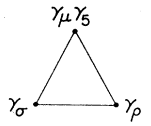

FIG. 1. Axial-vector triangle diagram which leads to the extra term in Eqs. (2) and (4).

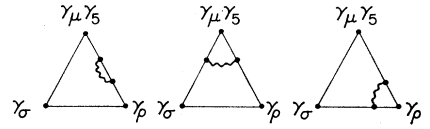

FIG. 2. Typical second-order radiative corrections to the triangle diagram in spinor electrodynamics.

* Research sponsored by the Air Force Office of Scientific Research, Office of Aerospace Research, U. S. Air Force, under AFOSR Grant No. 68-1365.

[1] S. L. Adler, Phys. Rev. **177**, 2426 (1969), hereafter referred to as I. As in I, we use the notation and metric conventions of J. D. Bjorken and S. D. Drell, *Relativistic Quantum Fields* (McGraw-Hill Book Co., New York, 1965), pp. 377–390.

[2] See also J. Schwinger, Phys. Rev. **82**, 664 (1951), Sec. V; C. R. Hagen, *ibid.* **177**, 2622 (1969); R. Jackiw and K. Johnson, *ibid.* **182**, 1459 (1969); R. A. Brandt, *ibid.* **180**, 1490 (1969); B. Zumino (unpublished).

[3] M. Gell-Mann and M. Lévy, Nuovo Cimento **16**, 705 (1960). We actually study a truncated version of the σ model proposed by J. S. Bell and R. Jackiw, *ibid.* **60A**, 47 (1969).

[4] For example, in order for the low-energy theorem for $\pi^0 \to 2\gamma$ derived in I to be valid, it is essential that there be no strong-interaction corrections to the anomalous term in Eq. (4).

II. GENERAL ARGUMENT

We develop in this section a general argument, valid to any finite order of perturbation theory, which shows that Eqs. (2) and (4) are exact. The basic idea is this: Since Eqs. (2) and (4) involve the *unrenormalized* fields, masses, and coupling constants, these equations are well defined only in a cutoff field theory. Consequently, for both of the field-theoretic models discussed, we construct a cutoff version by introducing photon or meson regulator fields with mass Λ. In both cases, the cutoff prescription allows the usual renormalization program to be carried out, so that the bare masses and couplings and the wave-function renormalizations are specified functions of the renormalized couplings and masses, and of the cutoff Λ. In the cutoff field theories, it is straightforward to prove the validity of Eqs. (2) and (4) for the unrenormalized quantities; this is our principal result. From Eqs. (2) and (4) we obtain exact low-energy theorems for the matrix elements $\langle 2\gamma|2im_0 j^5|0\rangle$ and $\langle 2\gamma|(-\mu_1{}^2/g_0)\pi|0\rangle$; the latter of these yields the $\pi^0\to 2\gamma$ low-energy theorem discussed in I.

Having summarized, in a very condensed way, our method and results, we now turn to the details in the various models.

A. Spinor Electrodynamics

We consider first the case of spinor electrodynamics, described by the Lagrangian density

$$\mathfrak{L}(x)=\bar\psi(x)(i\partial\!\!\!/-m_0)\psi(x)-\tfrac{1}{4}F_{\mu\nu}(x)F^{\mu\nu}(x) -e_0\bar\psi(x)\gamma_\mu\psi(x)A^\mu(x), \quad (5)$$

$$F_{\mu\nu}(x)=\partial_\nu A_\mu(x)-\partial_\mu A_\nu(x), \quad \partial\!\!\!/\equiv\gamma^\mu\partial_\mu.$$

We introduce a cutoff by modifying the usual Feynman rules for electrodynamics as follows.

(i) For each internal fermion line with momentum p we include a factor $i(p\!\!\!/-m_0+i\epsilon)^{-1}$ and for each vertex a factor $-ie_0\gamma_\mu$, with m_0 and e_0 the bare mass and charge. For each internal photon line of momentum q, we replace the usual propagator $-ig_{\mu\nu}(q^2+i\epsilon)^{-1}$ by the regulated propagator

$$-ig_{\mu\nu}\left(\frac{1}{q^2+i\epsilon}-\frac{1}{q^2-\Lambda^2+i\epsilon}\right)=\frac{-ig_{\mu\nu}}{q^2+i\epsilon}\frac{-\Lambda^2}{q^2-\Lambda^2+i\epsilon}. \quad (6)$$

(ii) Let $\Pi_{\mu\nu}{}^{(2)}(q)$ denote the two-vertex vacuum polarization loop [Fig. 3(a)]

$$\Pi_{\mu\nu}{}^{(2)}(q) =i\int\frac{d^4k}{(2\pi)^4}\mathrm{Tr}\left[\gamma_\mu\frac{1}{k\!\!\!/-m_0+i\epsilon}\gamma_\nu\frac{1}{k\!\!\!/+q\!\!\!/-m_0+i\epsilon}\right]. \quad (7)$$

Wherever $\Pi_{\mu\nu}{}^{(2)}(q)$ appears, we use its gauge-invariant, subtracted evaluation[5]

$$\Pi_{\mu\nu}{}^{(2)}(q)=(q_\mu q_\nu-g_{\mu\nu}q^2)\Pi^{(2)}(q^2), \quad \Pi^{(2)}(0)=0. \quad (8)$$

All vacuum polarization loops with four or more vertices [Fig. 3(b)] are calculated by imposing gauge invariance; this suffices to make them finite without need for further subtractions.

(iii) As usual, there is a factor $\int d^4l/(2\pi)^4$ for each internal integration over loop variable l and a factor -1 for each fermion loop.

(iv) We use the standard, iterative renormalization procedure[5] to fix the unrenormalized charge and mass e_0 and m_0 and the fermion wave-function renormalization Z_2 as functions of the renormalized charge and mass e and m and the cutoff Λ. For finite Λ, the renormalization constants e_0, m_0, and Z_2 will all be *finite*. The reason is that regulating the photon propagator (plus gauge invariance for loops) renders finite all vertex and electron self-energy parts and all photon self-energy parts other than $\Pi_{\mu\nu}{}^{(2)}$. [Examples of such vertex and self-energy parts are given in Fig. 3(c).] The self-energy part $\Pi_{\mu\nu}{}^{(2)}$ has already been made finite by explicit subtraction.

(v) We include wave-function renormalization factors $Z_2{}^{1/2}$ and $Z_3{}^{1/2}$ for each external fermion and photon line. (We recall that $Z_3=e^2/e_0{}^2$.)

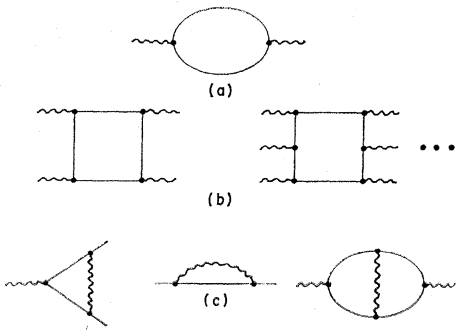

FIG. 3. (a) Two-vertex photon vacuum polarization loop. (b) Larger vacuum polarization loops. (c) Vertex and self-energy parts which are made finite by the photon propagator cutoff and gauge invariance of loops.

This simple set of rules makes all ordinary electrodynamics matrix elements finite. We may summarize the rules compactly by noting that they are the Feynman rules for the following *regulated* Lagrangian density:

$$\mathfrak{L}^R(x)=\mathfrak{L}_0{}^R(x)+\mathfrak{L}_I{}^R(x),$$

$$\mathfrak{L}_0{}^R(x)=\bar\psi(x)(i\partial\!\!\!/-m_0)\psi(x)-\tfrac{1}{4}F_{\mu\nu}(x)F^{\mu\nu}(x) +\tfrac{1}{4}F_{\mu\nu}{}^R(x)F^{R\mu\nu}(x)-\tfrac{1}{2}\Lambda^2A_\mu{}^R(x)A^{R\mu}(x), \quad (9)$$

$$\mathfrak{L}_I{}^R(x)=-e_0\bar\psi(x)\gamma_\mu\psi(x)[A^\mu(x)+A^{R\mu}(x)] +C^{(2)}[F_{\mu\nu}(x)+F_{\mu\nu}{}^R(x)][F^{\mu\nu}(x)+F^{R\mu\nu}(x)],$$

where $A_\mu{}^R$ is the field of the regulator vector meson of mass Λ, and $F_{\mu\nu}{}^R(x)=\partial_\nu A_\mu{}^R(x)-\partial_\mu A_\nu{}^R(x)$ is the regulator field strength tensor. The regulator field free

[5] Bjorken and Drell (Ref. 1), Chap. 19.

Lagrangian density is included in $\mathfrak{L}_0{}^R(x)$ with the opposite sign from normal; hence according to the canonical formalism, the regulator field is quantized with the opposite sign from normal—that is,

$$[A_\mu{}^R(x),\dot{A}_\nu{}^R(y)]|_{x^0=y^0}=ig_{\mu\nu}\delta^3(\mathbf{x}-\mathbf{y}),$$

whereas

$$[A_\mu(x),\dot{A}_\nu(y)]|_{x^0=y^0}=-ig_{\mu\nu}\delta^3(\mathbf{x}-\mathbf{y})$$

—giving the regulator bare propagator the opposite sign from the photon bare propagator. The interaction terms in $\mathfrak{L}_I{}^R(x)$ treat the regulator and the photon fields symmetrically. The term proportional to $C^{(2)}$ is a logarithmically infinite counter term which performs the explicit subtraction in the two-vertex vacuum polarization loop $\Pi_{\mu\nu}{}^{(2)}$, so that $\Pi^{(2)}(0)=0$.

Having specified our cutoff procedure, we are now ready to introduce the axial-vector and pseudoscalar currents $j_\mu{}^5(x)$ and $j^5(x)$, and to study their properties. First, we must check whether all matrix elements of these currents are finite when calculated in our cutoff theory. The answer is *yes*, that they are finite, and

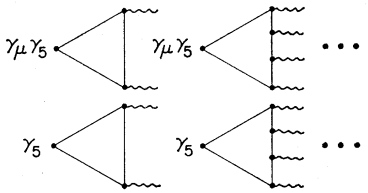

FIG. 4. Basic loops involving one axial-vector or one pseudoscalar vertex.

follows immediately from the fact that all of the basic fermion loops involving one axial-vector or one pseudoscalar vertex (Fig. 4) are made finite by the imposition of gauge invariance on the photon vertices, without the need for explicit subtractions. Thus, we can turn immediately to the problem of showing that Eq. (2) is exactly satisfied in our cutoff theory.

Let us consider an arbitrary Feynman amplitude involving $j_\mu{}^5$, with $2f$ external fermion and b external boson lines (Fig. 5). Proceeding as in I, we divide the diagrams contributing to the Feynman amplitude into two categories, which we call type (a) and type (b). The type-(a) diagrams are those in which the axial-vector vertex $\gamma_\mu\gamma_5$ is attached to one of the f fermion lines running through the diagram; a typical type-(a) contribution is shown in Fig. 6(a). By contrast, the type-(b) diagrams are those in which the axial-vector vertex $\gamma_\mu\gamma_5$ is attached to an internal closed loop; in Fig. 6(b) we show a typical contribution of type (b). In both Figs. 6(a) and 6(b), we have denoted by Q the four-momentum carried by the axial-vector current.

To study the divergence of the axial-vector current, we multiply the matrix element of $j_\mu{}^5$ by iQ^μ. We turn

FIG. 5. Arbitrary Feynman amplitude involving $j_\mu{}^5$.

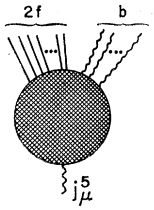

our attention first to the type-(a) contribution pictured in Fig. 6(a), which can be written

$$\sum_{k=1}^{2n-1}\prod_{j=1}^{k-1}\left[\gamma^{(j)}\frac{1}{p+p_j-m_0}\right]\gamma^{(k)}\frac{1}{p+p_k-m_0}\gamma_\mu\gamma_5\frac{1}{p'+p_k-m_0}\times\prod_{j=k+1}^{2n-1}\left[\gamma^{(j)}\frac{1}{p'+p_j-m_0}\right]\gamma^{(2n)}(\cdots),\quad(10)$$

$$Q=p-p',$$

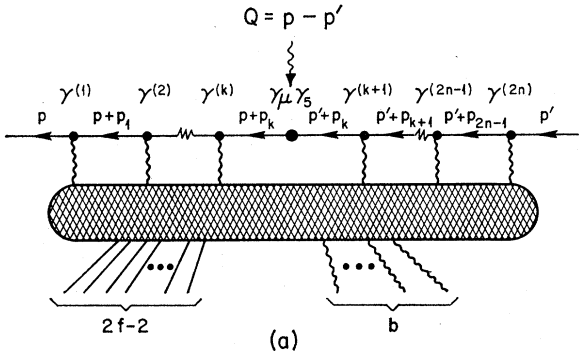

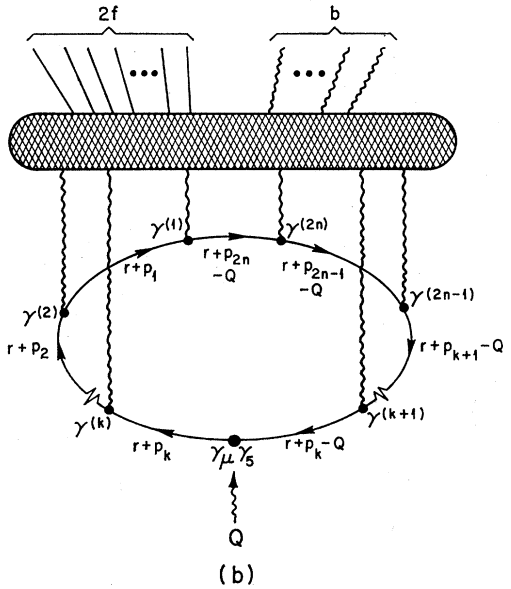

FIG. 6. (a) Contribution to Fig. 5 in which the axial-vector vertex is attached to one of the f fermion lines running through the diagram. (b) Contribution to Fig. 5 in which the axial-vector vertex is attached to an internal closed loop.

where we have focused our attention on the line to which the $\gamma_\mu\gamma_5$ vertex is attached and have denoted the remainder of the diagram by $(\cdots)$. As shown in I, when we multiply the propagator string in Eq. (10) by iQ^μ and do an algebraic rearrangement of terms, we obtain the following identity:

$$iQ^\mu \sum_{k=1}^{2n-1} \prod_{j=1}^{k-1} \left[\gamma^{(j)} \frac{1}{p+p_j-m_0}\right] \gamma^{(k)} \frac{1}{p+p_k-m_0} \gamma_\mu\gamma_5 \frac{1}{p'+p_k-m_0} \prod_{j=k+1}^{2n-1} \left[\gamma^{(j)} \frac{1}{p'+p_j-m_0}\right] \gamma^{(2n)}$$

$$= \sum_{k=1}^{2n-1} \prod_{j=1}^{k-1} \left[\gamma^{(j)} \frac{1}{p+p_j-m_0}\right] \gamma^{(k)} \frac{1}{p+p_k-m_0} 2im_0\gamma_5 \frac{1}{p'+p_k-m_0} \prod_{j=k+1}^{2n-1} \left[\gamma^{(j)} \frac{1}{p'+p_j-m_0}\right] \gamma^{(2n)}$$

$$-i \prod_{j=1}^{2n-1} \left[\gamma^{(j)} \frac{1}{p+p_j-m_0}\right] \gamma^{(2n)}\gamma_5 - i\gamma_5 \prod_{j=1}^{2n-1} \left[\gamma^{(j)} \frac{1}{p'+p_j-m_0}\right] \gamma^{(2n)}. \quad (11)$$

Since the integrals over the four-momenta of the photon propagators joining the fermion propagator string to the "blob" in Fig. 6(a) (i.e., the integrals over $p_1,\cdots,p_{2n-1}$) are all *convergent* in our regulated field theory, it is safe to do the algebraic manipulations implicit in Eq. (11) *inside* the integrals. The first term on the right-hand side of Eq. (11) gives the type-(a) contribution to the Feynman amplitude for $2im_0j^5$, corresponding to replacing $\gamma_\mu\gamma_5$ by $2im_0\gamma_5$ in Fig. 6(a). The two remaining terms in Eq. (11) are the usual "surface terms" which arise in Ward identities from the equal-time commutator of $j_0{}^5$ with the fields of the external fermions of momenta p and p'.[6] Thus, as far as the type-(a) contributions to the Feynman amplitude are concerned, the divergence of $j_\mu{}^5$ is simply $2im_0j^5$, with no extra terms present.

We turn next to the type-(b) contribution pictured in Fig. 6(b), which we write as

$$L(Q;\gamma_\mu\gamma_5;p_1,\cdots,p_{2n-1})(\cdots),$$

$$L(Q;\Gamma;p_1,\cdots,p_{2n-1})$$

$$= \int d^4r \,\mathrm{Tr}\left\{\sum_{k=1}^{2n} \prod_{j=1}^{k-1} \left[\gamma^{(j)} \frac{1}{r+p_j-m_0}\right] \times \gamma^{(k)} \frac{1}{r+p_k-m_0} \Gamma \frac{1}{r+p_k-Q-m_0} \times \prod_{j=k+1}^{2n} \left[\gamma^{(j)} \frac{1}{r+p_j-Q-m_0}\right]\right\}, \quad (12)$$

where we have focused our attention on the closed loop and have again denoted the remainder of the diagram by $(\cdots)$. As was shown in I, some straightforward algebra implies

$$L(Q;iQ^\mu\gamma_\mu\gamma_5;p_1,\cdots,p_{2n-1})$$

$$= L(Q;2im_0\gamma_5;p_1,\cdots,p_{2n-1})$$

$$+ i\int d^4r \,\mathrm{Tr}\left\{\gamma_5 \prod_{j=1}^{2n} \left[\gamma^{(j)} \frac{1}{r+p_j-m_0}\right] - \gamma_5 \prod_{j=1}^{2n} \left[\gamma^{(j)} \frac{1}{r+p_j-Q-m_0}\right]\right\}. \quad (13)$$

For loops with $n\geq 2$ (i.e., with four or more vector vertices) the residual integral in Eq. (13) is sufficiently convergent for us to be able to make the change of variable $r\rightarrow r+Q$ in the second term, causing the two terms in the curly brackets to cancel. Thus, the loops with $n\geq 2$ satisfy the usual Ward identity

$$L(Q;iQ^\mu\gamma_\mu\gamma_5;p_1,\cdots,p_{2n-1}) = L(Q;2im_0\gamma_5;p_1,\cdots,p_{2n-1}). \quad (14)$$

Again, since the integrals over $p_1,\cdots,p_{2n-1}$ are all *convergent* in the regulated field theory, the manipulations leading to Eq. (14) can all be performed *inside* these integrals. This means that the type-(b) pieces containing loops with $n\geq 2$ all agree with the usual divergence equation $\partial^\mu j_\mu{}^5(x)=2im_0j^5(x)$.

Finally, we must consider the case $n=1$, that is, the axial-vector triangle diagram illustrated in Fig. 7. As was shown in I, when the triangle is defined to be gauge-invariant with respect to the vector indices, it does *not* satisfy Eq. (14) for the axial-vector index divergence. Instead, there is a well-defined extra term left over which comes from the failure of the two terms in the curly brackets in Eq. (13) to cancel. The analysis of I shows that the effect of the extra term is to add to the normal axial-vector divergence equation the term

$$(\alpha_0/4\pi)[F^{\xi\sigma}(x)+F^{R\xi\sigma}(x)] \times [F^{\tau\rho}(x)+F^{R\tau\rho}(x)]\epsilon_{\xi\sigma\tau\rho}. \quad (15)$$

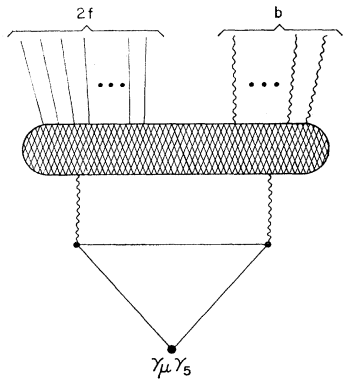

FIG. 7. Contribution of the axial-vector triangle diagram to the Feynman amplitude of Fig. 5.

[6] Y. Takahashi, Nuovo Cimento **6**, 370 (1957).

To summarize, our diagrammatic analysis shows that the axial-vector divergence equation in the regulated field theory is

$$\partial^\mu j_\mu{}^5(x) = 2im_0 j^5(x) + (\alpha_0/4\pi) F^{\xi\sigma}(x) F^{\tau\rho}(x) \epsilon_{\xi\sigma\tau\rho} + (\alpha_0/4\pi)[F^{\xi\sigma}(x) F^{R\tau\rho}(x) + F^{R\xi\sigma}(x) F^{\tau\rho}(x) + F^{R\xi\sigma}(x) F^{R\tau\rho}(x)] \epsilon_{\xi\sigma\tau\rho}. \quad (16)$$

Equation (16) is identical with Eq. (2), apart from the terms involving F^R which arise from our explicit inclusion of a regulator field. The crucial point is that the coefficient of the anomalous term is exactly $\alpha_0/4\pi$ and *does not involve an unknown power series in the coupling constant coming from higher orders in perturbation theory.*

The diagrammatic analysis which we have just given may be rephrased succinctly as follows: If we use the regulated Lagrangian density in Eq. (9) to calculate equations of motion, and then use the equations of motion to naively calculate the axial divergence, we find

$$\partial^\mu j_\mu{}^5(x) = 2im_0 j^5(x). \quad (17)$$

Extra terms on the right-hand side of Eq. (17) can only come from singular diagrams where the naive derivation breaks down. In the regulated field theory, all virtual photon integrations *converge* and therefore, cannot lead to singularities giving additional terms in Eq. (17). Hence breakdown in Eq. (17) (if it occurs at all) must be associated with the basic axial-vector loops shown in Fig. 4. But, as we have seen, the axial-vector loops with four or more photons satisfy Eq. (17), so the basic triangle diagram is the *only* possible source of an anomaly.

Having derived our basic result, we turn next to the low-energy theorem for $2im_0 j^5(x)$ which is implied by Eq. (16). Taking the matrix element of Eq. (16) between a state with two photons and the vacuum gives

$$F(k_1\cdot k_2) = G(k_1\cdot k_2) + H(k_1\cdot k_2), \quad (18)$$

where

$$\langle\gamma(k_1,\epsilon_1)\gamma(k_2,\epsilon_2)|\,\partial^\mu j_\mu{}^5|0\rangle = (4k_{10}k_{20})^{-1/2} k_1{}^\xi k_2{}^\tau \epsilon_1{}^{*\sigma} \epsilon_2{}^{*\rho} \epsilon_{\xi\tau\sigma\rho} F(k_1\cdot k_2),$$

$$\langle\gamma(k_1,\epsilon_1)\gamma(k_2,\epsilon_2)|\,2im_0 j^5|0\rangle = (4k_{10}k_{20})^{-1/2} k_1{}^\xi k_2{}^\tau \epsilon_1{}^{*\sigma} \epsilon_2{}^{*\rho} \epsilon_{\xi\tau\sigma\rho} G(k_1\cdot k_2),$$

$$(\alpha_0/4\pi)\langle\gamma(k_1,\epsilon_1)\gamma(k_2,\epsilon_2)|\,(F^{\xi\sigma}+F^{R\xi\sigma})(F^{\tau\rho}+F^{R\tau\rho})\epsilon_{\xi\sigma\tau\rho}|0\rangle = (4k_{10}k_{20})^{-1/2} k_1{}^\xi k_2{}^\tau \epsilon_1{}^{*\sigma} \epsilon_2{}^{*\rho} \epsilon_{\xi\tau\sigma\rho} H(k_1\cdot k_2). \quad (19)$$

We wish, in particular, to study Eq. (18) at the point $k_1\cdot k_2=0$. As has been shown by Sutherland and Veltman,[7] $F(k_1\cdot k_2) \propto k_1\cdot k_2$, so the left-hand side of Eq. (18) vanishes at $k_1\cdot k_2=0$, giving

$$G(0) = -H(0). \quad (20)$$

There are two types of diagrams which contribute to $H(k_1\cdot k_2)$, as illustrated in Fig. 8, where we have used the symbol ⊗ to denote action of the operator

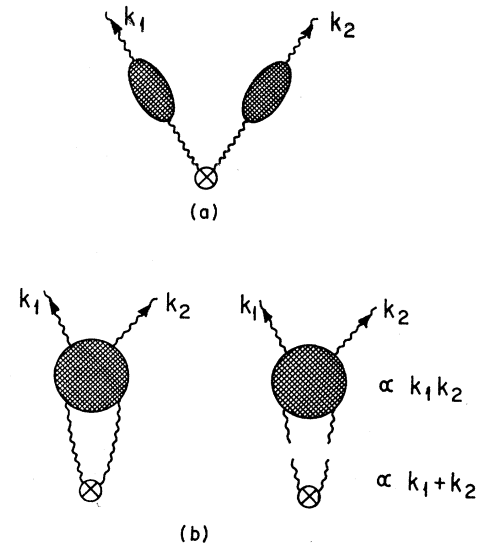

FIG. 8. (a) Diagram in which the operator $(\alpha_0/4\pi)(F^{\xi\sigma}+F^{R\xi\sigma}) \times (F^{\tau\rho}+F^{R\tau\rho})\epsilon_{\xi\sigma\tau\rho}$, denoted by ⊗, attaches directly to the external photon lines. (b) Diagram in which there is a photon-photon scattering between ⊗ and the two external photons.

$(\alpha_0/4\pi)(F^{\xi\sigma}+F^{R\xi\sigma})(F^{\tau\rho}+F^{R\tau\rho})\epsilon_{\xi\sigma\tau\rho}$. In the diagrams in Fig. 8(a), the field strength operators attach directly onto the external photon lines, without photon-photon scattering. The effect of the vacuum polarization parts and the external-line wave-function renormalizations is to change α_0 to α, giving

$$H(0)^{(a)} = 2\alpha/\pi. \quad (21)$$

In the diagrams in Fig. 8(b), there is a photon-photon scattering between ⊗ and the free photons. As a result of the antisymmetric tensor structure of the anomalous divergence term, the vertex ⊗ is proportional to k_1+k_2. Also, the diagram for the scattering of light by light is itself proportional to k_1k_2, since photon gauge invariance implies that the external photons couple through their field strength tensors.[8] Thus, the diagrams in Fig. 8(b) are proportional to $k_1k_2(k_1+k_2)$ and are of higher order than the terms which contribute to the low-energy theorem, giving us

$$H(0)^{(b)} = 0. \quad (22)$$

Combining Eqs. (20)–(22), we get an *exact low-energy theorem* for the operator $2im_0 j^5$,

$$G(0) = -2\alpha/\pi. \quad (23)$$

So far in our discussion we have kept the cutoff Λ finite, so that $G(0)$ is a matrix element calculated with our modified Feynman rules. Let us now indicate briefly the form which Eq. (23) takes when the cutoff Λ becomes infinite. A straightforward analysis of matrix elements of the operator j^5 shows that divergences as $\Lambda \to \infty$ are associated *only* with the electron propagator

[7] D. G. Sutherland, Nucl. Phys. **B2**, 433 (1967).

[8] R. Karplus and M. Neumann, Phys. Rev. **80**, 380; **83**, 776 (1950).

$S_F'(p)$, the photon propagator $D_F'(q)_{\mu\nu}$, the photon vertex part $\Gamma_\mu(p,p')$, and, in addition, the pseudoscalar vertex part $\Gamma^5(p,p')$, defined by

$$S_F'(p)\Gamma^5(p,p')S_F'(p') = -\int d^4x d^4y\, e^{ip\cdot x}e^{-ip'\cdot y} \times\langle T(\psi(x)j^5(0)\bar{\psi}(y))\rangle_0. \quad (24)$$

In matrix elements of $m_0 j^5$, the vertex part $\Gamma^5(p,p')$ will clearly always occur in the combination $m_0\Gamma^5(p,p')$. Let us now introduce the usual electrodynamic renormalizations

$$\begin{aligned} Z_2^{-1}S_F'(p) &= \tilde{S}_F'(p), \\ Z_3^{-1}D_F'(q)_{\mu\nu} &= \tilde{D}_F'(q)_{\mu\nu}, \\ Z_1\Gamma_\mu(p,p') &= \tilde{\Gamma}_\mu(p,p'), \\ Z_1 = Z_2, \quad e_0 &= Z_3^{-1/2}e, \end{aligned} \quad (25)$$

plus the usual wave-function renormalizations on external lines. The effect of these rescalings is to replace $m_0\Gamma^5(p,p')$, wherever it occurs, by $m_0Z_2\Gamma^5(p,p')$. But, as we will now show, this latter quantity is *finite* (i.e., cutoff-independent as $\Lambda\to\infty$). To see this, we note first that $\Gamma^5(p,p')$ is multiplicatively renormalizable[9]; therefore, if $Z_5\Gamma^5(p,p)$ is finite, then so is $Z_5\Gamma^5(p,p')$. Next, let us write the Ward identity for the axial-vector vertex,

$$(p-p')^\mu\Gamma_\mu{}^5(p,p') = 2m_0\Gamma^5(p,p') - i(\alpha_0/4\pi)\tilde{F}(p,p') + S_F'(p)^{-1}\gamma_5 + \gamma_5 S_F'(p')^{-1}, \quad (26)$$

where $\Gamma_\mu{}^5$ and $\tilde{F}$ are defined by replacing $j^5(0)$ in Eq. (24) by $j_\mu{}^5(0)$ and $F^{\xi\sigma}(0)F^{\tau\rho}(0)\epsilon_{\xi\sigma\tau\rho}$, respectively. When $p=p'$, the left-hand side of Eq. (26) obviously vanishes. It is also easy to see that $\tilde{F}(p,p)=0$ as a result of the antisymmetric tensor structure of this term. So the axial-vector Ward identity at $p=p'$ becomes the simple equation

$$0 = 2m_0\Gamma^5(p,p) + S_F'(p)^{-1}\gamma_5 + \gamma_5 S_F'(p)^{-1}, \quad (27)$$

which immediately implies that $m_0Z_2\Gamma^5(p,p)$ is finite. If we introduce a renormalized pseudoscalar vertex part by writing

$$m_0Z_2\Gamma^5(p,p') = m\tilde{\Gamma}^5(p,p'), \quad (28)$$

then Eq. (28) may be rewritten as the equal-momentum boundary condition

$$0 = 2m\tilde{\Gamma}^5(p,p) + \tilde{S}_F'(p)^{-1}\gamma_5 + \gamma_5\tilde{S}_F'(p)^{-1}. \quad (29)$$

The results of this analysis may be summarized as follows: If we calculate an arbitrary matrix element of $m_0 j^5$ in our cutoff theory, and then let $\Lambda\to\infty$, we get the same answer as if we calculated all the skeleton diagrams for the matrix element and replaced the electron and photon lines and the vertex parts appearing in the skeleton by the renormalized quantities $\tilde{S}_F'(p)$, $\tilde{D}_F'(q)_{\mu\nu}$, $\tilde{\Gamma}_\mu(p,p')$, and $m\tilde{\Gamma}^5(p,p')$. These quantities can all be calculated without recourse to cutoffs by using dispersive methods; in the case of the pseudoscalar vertex the subtraction constant in the dispersion relation can be fixed by using Eq. (29) as a boundary condition.

Returning to our low-energy theorem, we see that in the limit $\Lambda\to\infty$ the pseudoscalar-photon-photon matrix element $G(k_1\cdot k_2)$ becomes the renormalized matrix element $\tilde{G}(k_1\cdot k_2)$ calculated by the recipe we have just outlined, and the low-energy theorem tells us that

$$\tilde{G}(0) = -2\alpha/\pi. \quad (30)$$

In other words, all order α^2, α^3, $\cdots$, contributions to $\tilde{G}(k_1\cdot k_2)$ vanish at $k_1\cdot k_2=0$. In the next section, we will verify by explicit calculation that the order α^2 terms do cancel.

In conclusion, we remark that the arguments which we have given in this section for spinor electrodynamics apply, with only trivial modification, to the neutral-vector-meson model of strong interactions. In particular the low-energy theorem analogous to Eq. (23) will hold to all orders in both α and the neutral-vector-meson strong coupling.

B. σ Model

We turn next to the case of Gell-Mann and Lévy's σ model.[3] As in I, we consider a truncated version of the σ model which contains only a proton (ψ), a neutral pion (π), and a scalar meson (σ), but omits the charged pions and the neutron. Our exposition will differ somewhat from the previous case of spinor electrodynamics, where we *first* introduced a cutoff procedure to remove infinities from the theory, and then afterwards proceeded to discuss the properties of the axial-vector current. In the case of the σ model, we will have to consider the axial-vector current *simultaneously* with our introduction of the cutoff, in order to ensure that the cutoff preserves the usual PCAC equation [Eq. (3)] when electromagnetic interactions are neglected. Once we are sure that the axial-vector divergence equation in the absence of electromagnetism has no abnormalities, we can then determine how Eq. (3) is modified when electromagnetic effects are taken into account.

We begin by writing the Lagrangian for the σ model and discussing some of the formal properties of this theory. We have

$$\begin{aligned} \mathfrak{L} = {} & \bar{\psi}[i\partial - G_0(g_0^{-1}+\sigma+i\pi\gamma_5)]\psi \\ & + \lambda_0[4\sigma^2 + 4g_0\sigma(\sigma^2+\pi^2) + g_0^2(\sigma^2+\pi^2)^2] \\ & + \tfrac{1}{2}\mu_0{}^2[2g_0^{-1}\sigma + \sigma^2 + \pi^2] \\ & + \tfrac{1}{2}[(\partial\pi)^2 + (\partial\sigma)^2] - \tfrac{1}{2}\mu_1{}^2(\pi^2+\sigma^2), \end{aligned} \quad (31)$$

[9] We recall that multiplicative renormalizability of the usual vector vertex Γ_ρ follows from the fact that Γ_ρ satisfies the integral equation $\Gamma_\rho = \gamma_\rho - \int\Gamma_\rho S_F'S_F'K$ [see Bjorken and Drell (Ref. 5)]. More generally, G. Preparata and W. I. Weisberger [Phys. Rev. **175**, 1965 (1968)] have observed that in spinor electrodynamics the vertex $\Gamma_O(p,p')$ of $\bar{\psi}O\psi$, with O a product of γ-matrices, satisfies the integral equation $\Gamma_O = O - \int\Gamma_O S_F'S_F'K$, and therefore is multiplicatively renormalizable.

where we have chosen the fully translated form of the σ model with

$$\langle\sigma\rangle_0=0 \tag{32}$$

to all orders of perturbation theory. The axial-vector current is generated by the chiral gauge transformation

$$\begin{aligned}\psi &\longrightarrow (1+\tfrac{1}{2}i\gamma_5 v)\psi\,,\\ \pi &\longrightarrow \pi-v(g_0^{-1}+\sigma)\,,\\ g_0^{-1}+\sigma &\longrightarrow g_0^{-1}+\sigma+v\pi\,,\end{aligned} \tag{33}$$

giving

$$\begin{aligned}&j_\mu{}^5=-\delta\mathfrak{L}/\delta(\partial^\mu v)=\bar\psi\tfrac{1}{2}\gamma_\mu\gamma_5\psi+\sigma\partial_\mu\pi-\pi\partial_\mu\sigma+g_0^{-1}\partial_\mu\pi\,,\\ &\partial^\mu j_\mu{}^5=-\delta\mathfrak{L}/\delta v=-(\mu_1{}^2/g_0)\pi\,.\end{aligned} \tag{34}$$

The terms in Eq. (31) have the following significance: (i) G_0 is the unrenormalized meson-nucleon coupling constant; (ii) the quantity g_0 is related to the bare nucleon mass m_0 by

$$G_0/g_0=m_0\,, \tag{35}$$

and may be expressed directly as a vacuum expectation value,

$$1/g_0=i\left\langle\left[\int d^3x\; j_0{}^5(x),\pi(0)\right]\right|_{x_0=0}\Bigg\rangle_0\,; \tag{36}$$

(iii) $\mu_1{}^2$ is the bare meson mass which appears in the bare propagators $\Delta_F{}^\sigma(q)$ and $\Delta_F{}^\pi(q)$,

$$\Delta_F{}^{\sigma,\pi}(q)=1/(q^2-\mu_1{}^2+i\epsilon)\,; \tag{37}$$

(iv) the term $\lambda_0[4\sigma^2+4g_0\sigma(\sigma^2+\pi^2)+g_0{}^2(\sigma^2+\pi^2)^2]$ is a chiral-invariant meson-meson scattering interaction; and (v) the term $\frac{1}{2}\mu_0{}^2[2g_0{}^{-1}\sigma+\sigma^2+\pi^2]$ is a chiral-invariant *counter term* which is necessary to guarantee that

$$\langle\delta\mathfrak{L}/\delta\sigma\rangle_0=\partial_\lambda\langle\delta\mathfrak{L}/\delta(\partial_\lambda\sigma)\rangle_0=0\,, \tag{38}$$

as is required by the Euler-Lagrange equations of motion and translation invariance. Equations (32) and (38) fix $\mu_0{}^2$ to have the value

$$\mu_0{}^2=\langle G_0 g_0\bar\psi\psi-\lambda_0[4g_0{}^2(3\sigma^2+\pi^2)+4g_0{}^3\sigma(\sigma^2+\pi^2)]\rangle_0\,. \tag{39}$$

The effect of $\mu_0{}^2$, which is formally quadratically divergent, is to remove the "tadpole" diagrams of the type shown in Fig. 9, so that the condition $\langle\sigma\rangle_0=0$ is maintained in each order of perturbation theory. It is easily seen that the $\mu_0{}^2$ counter term simultaneously removes the quadratically divergent parts of the π- and σ-meson self-energies, so that the remaining bare quantities appearing in the Lagrangian (G_0,g_0,μ_1), as well as the wave-function renormalizations, are at most *logarithmically* divergent.

FIG. 9. Tadpole diagram.

An important feature of the Lagrangian density in Eq. (31) is that it is *not* normal-ordered; the omission of normal ordering is essential in order for the axial-vector current to satisfy the PCAC equation (34). To see this, let us consider the effect of normal ordering on the chiral-invariant meson-meson scattering term,

$$\begin{aligned}&\mathfrak{L}_{MM}=\mathfrak{L}_{MM}{}^{(2)}+\mathfrak{L}_{MM}{}^{(3)}+\mathfrak{L}_{MM}{}^{(4)}\,,\\ &\mathfrak{L}_{MM}{}^{(2)}=4\sigma^2\,,\quad \mathfrak{L}_{MM}{}^{(3)}=4g_0\sigma(\sigma^2+\pi^2)\,,\\ &\mathfrak{L}_{MM}{}^{(4)}=g_0{}^2(\sigma^2+\pi^2)^2\,.\end{aligned} \tag{40}$$

The normal-ordered forms of the two-, three-, and four-meson scattering terms are defined by

$$\begin{aligned}&\langle:\mathfrak{L}_{MM}{}^{(2)}:\rangle_0=\langle(\partial/\partial\sigma):\mathfrak{L}_{MM}{}^{(2)}:\rangle=0\,,\\ &\langle:\mathfrak{L}_{MM}{}^{(3)}:\rangle_0=\langle(\partial/\partial\sigma):\mathfrak{L}_{MM}{}^{(3)}:\rangle_0=\langle(\partial/\partial\pi):\mathfrak{L}_{MM}{}^{(3)}:\rangle_0\\ &\qquad=\langle(\partial^2/\partial\sigma^2):\mathfrak{L}_{MM}{}^{(3)}:\rangle_0\\ &\qquad=\langle(\partial/\partial\sigma)(\partial/\partial\pi):\mathfrak{L}_{MM}{}^{(3)}:\rangle_0\\ &\qquad=\langle(\partial^2/\partial\pi^2):\mathfrak{L}_{MM}{}^{(3)}:\rangle_0=0\,,\\ &\langle:\mathfrak{L}_{MM}{}^{(4)}:\rangle_0=\langle(\partial/\partial\sigma):\mathfrak{L}_{MM}{}^{(4)}:\rangle_0=\langle(\partial/\partial\pi):\mathfrak{L}_{MM}{}^{(4)}:\rangle_0\\ &\qquad=\langle(\partial^2/\partial\sigma^2):\mathfrak{L}_{MM}{}^{(4)}:\rangle_0=\cdots\\ &\qquad=\langle(\partial^3/\partial\pi^3):\mathfrak{L}_{MM}{}^{(4)}:\rangle_0=0\,.\end{aligned} \tag{41}$$

These conditions may easily be satisfied by introducing counter terms to remove the vacuum expectation values of the various derivatives,

$$\begin{aligned}&:\mathfrak{L}_{MM}{}^{(2)}:=4\sigma^2-\langle4\sigma^2\rangle_0\,,\\ &:\mathfrak{L}_{MM}{}^{(3)}:=4g_0\sigma(\sigma^2+\pi^2)-4g_0\sigma\langle3\sigma^2+\pi^2\rangle_0\\ &\qquad\qquad-4g_0\langle\sigma(\sigma^2+\pi^2)\rangle_0\,,\\ &:\mathfrak{L}_{MM}{}^{(4)}:=g_0{}^2(\sigma^2+\pi^2)^2-4g_0{}^2\sigma\langle\sigma(\sigma^2+\pi^2)\rangle_0\\ &\qquad-2g_0{}^2\sigma^2\langle3\sigma^2+\pi^2\rangle_0-2g_0{}^2\pi^2\langle\sigma^2+3\pi^2\rangle_0\\ &\qquad-g_0{}^2\langle(\sigma^2+\pi^2)^2\rangle_0+2g_0{}^2\langle\sigma^2\rangle_0\langle3\sigma^2+\pi^2\rangle_0\\ &\qquad\qquad+2g_0{}^2\langle\pi^2\rangle_0\langle\sigma^2+3\pi^2\rangle_0\,,\end{aligned} \tag{42}$$

giving

$$\begin{aligned}:\mathfrak{L}_{MM}:=&\mathfrak{L}_{MM}-4g_0\sigma\langle3\sigma^2+\pi^2\rangle_0-4g_0{}^2\sigma\langle\sigma(\sigma^2+\pi^2)\rangle_0\\ &-2g_0{}^2\sigma^2\langle3\sigma^2+\pi^2\rangle_0-2g_0{}^2\pi^2\langle\sigma^2+3\pi^2\rangle_0\\ &+\text{const}.\end{aligned} \tag{43}$$

Clearly, the normal-ordered interaction $:\mathfrak{L}_{MM}:$ will be chiral-invariant only if the counter terms combine to be proportional to $\sigma^2+\pi^2+2\sigma/g_0$, that is, only if

$$\langle3\sigma^2+\pi^2\rangle_0=\langle\sigma^2+3\pi^2\rangle_0=\langle3\sigma^2+\pi^2\rangle_0+g_0\langle\sigma(\sigma^2+\pi^2)\rangle_0\,, \tag{44}$$

which requires

$$\begin{aligned}&\langle\sigma^2\rangle_0=\langle\pi^2\rangle_0\,,\\ &\langle\sigma(\sigma^2+\pi^2)\rangle_0=0\,.\end{aligned} \tag{45}$$

These conditions would be satisfied if π and σ were free fields, but they are *not* true in the presence of the interaction terms of Eq. (31). Thus, the normal-ordered form $:\mathfrak{L}_{MM}:$ is not invariant under the chiral gauge transformation of Eq. (33) and, if used in the Lagrangian instead of $\mathfrak{L}_{MM}$, spoils the PCAC equation. The way out of this difficulty consists in noting that the

normal-ordering conditions of Eq. (4) are not necessary for the consistency of the Lagrangian field theory of Eq. (31); all that is necessary is the single condition $\langle\delta\mathfrak{L}/\delta\sigma\rangle_0=0$. As we have seen, this condition can be satisfied by including the chiral-invariant counter term proportional to μ_0^2, without any use of normal ordering in the Lagrangian.

The fact that μ_0^2 removes the quadratic divergence from the π and σ self-energies can be expressed in a simple equation, which will be very useful in what follows. Let $\Delta_F^{\pi'}(q)$ denote the full pion propagator, given by

$$\Delta_F^{\pi'}(q)=-i\int d^4x\, e^{iq\cdot x}\langle T(\pi(x)\pi(0))\rangle_0$$
$$=1/[q^2-\mu_1^2-\Sigma^\pi(q^2)], \tag{46}$$

where $\Sigma^\pi(q^2)$ is the pion proper self-energy. According to Eq. (46),

$$\Delta_F^{\pi'}(0)=-1/[\mu_1^2+\Sigma^\pi(0)]. \tag{47}$$

An alternative expression for $\Delta_F^{\pi'}(q)$ may be obtained by substituting the PCAC equation (34) into Eq. (46),

$$\Delta_F^{\pi'}(q)=i\frac{g_0}{\mu_1^2}\int d^4x\, e^{iq\cdot x}\langle T((\partial/\partial x_\mu)j_\mu^5(x)\pi(0))\rangle_0$$
$$=\frac{g_0}{\mu_1^2}q^\mu\int d^4x\, e^{iq\cdot x}\langle T(j_\mu^5(x)\pi(0))\rangle_0$$
$$-\frac{ig_0}{\mu_1^2}\int d^3x\, e^{-iq\cdot x}\langle[j_0^5(x),\pi(0)]|_{x_0=0}\rangle_0, \tag{48}$$

which at $q=0$ becomes

$$\Delta_F^{\pi'}(0)=-\frac{ig_0}{\mu_1^2}\int d^3x\,\langle[j_0^5(x),\pi(0)]|_{x_0=0}\rangle_0=\frac{-1}{\mu_1^2}. \tag{49}$$

Comparing Eqs. (47) and (49), we obtain the desired result

$$\Sigma^\pi(0)=0. \tag{50}$$

Since the differences $\Sigma^\pi(q^2)-\Sigma^\pi(0)$ and $\Sigma^\sigma(q^2)-\Sigma^\pi(0)$ are only logarithmically divergent, Eq. (50) tells us that the π and σ self-energies $\Sigma^\pi(q^2)$ and $\Sigma^\sigma(q^2)$ are themselves only logarithmically divergent.

So far, we have discussed the σ model in the absence of electromagnetism. To include electromagnetism, we add to the Lagrangian density of Eq. (31) the terms

$$-\tfrac{1}{4}F_{\mu\nu}F^{\mu\nu}-e_0\bar\psi\gamma_\mu\psi A^\mu. \tag{51}$$

We expect, because of the presence of triangle diagrams, that electromagnetism will modify the PCAC equation by the addition of a term proportional to $F^{\xi\sigma}F^{\tau\rho}\epsilon_{\xi\sigma\tau\rho}$. However, it is easy to see that all of the other formal properties of the σ model which we have derived above are unchanged. In particular, *Eq. (50) is still valid in the presence of electromagnetism*, since the antisymmetric tensor structure of the extra term in the PCAC equation causes the contribution of this term to Eq. (48) to vanish at $q=0$.

This completes our survey of the formal properties of the σ model. We proceed to introduce a cutoff (with electromagnetism included) by modifying the usual Feynman rules as follows.

(i) For each internal fermion line with momentum p we include a factor $i(\not p-m_0+i\epsilon)^{-1}$, with $m_0=G_0/g_0$. For each internal photon line of momentum q, we replace the usual propagator $-ig_{\mu\nu}(q^2+i\epsilon)^{-1}$ by the regulated propagator

$$-ig_{\mu\nu}\left(\frac{1}{q^2+i\epsilon}-\frac{1}{q^2-\Lambda^2+i\epsilon}\right)=\frac{-ig_{\mu\nu}}{q^2+i\epsilon}\left(\frac{-\Lambda^2}{q^2-\Lambda^2+i\epsilon}\right). \tag{52}$$

For internal π or σ lines, *which are not attached at either end to the axial-vector current*, we replace the usual propagator $i(q^2-\mu_1^2+i\epsilon)^{-1}$ by the regulated propagator

$$i\left(\frac{1}{q^2-\mu_1^2+i\epsilon}-\frac{1}{q^2-\Lambda^2+i\epsilon}\right)$$
$$=\frac{i}{q^2-\mu_1^2+i\epsilon}\left(\frac{-\Lambda^2+\mu_1^2}{q^2-\Lambda^2+i\epsilon}\right). \tag{53}$$

For the photon-nucleon, meson-nucleon, and meson-meson vertices, we include the factors shown in Fig. 10, with e_0, g_0, G_0, and λ_0 the appropriate bare couplings.

(ii) For the axial-vector-current–nucleon and axial-vector-current–meson vertices, we include the factors shown in Fig. 11. For the pion propagator immediately following the axial-vector-current–pion vertex, we use the *unregulated* propagator $i(q^2-\mu_1^2+i\epsilon)^{-1}$, while we replace the *product* of pion and σ propagators immediately following the axial-vector-current–pion–σ

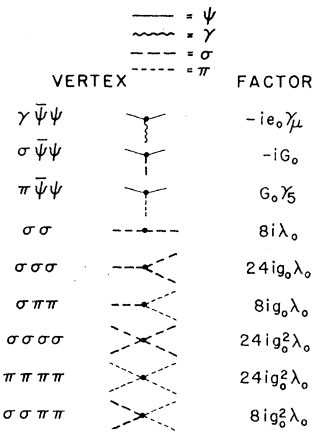

FIG. 10. Feynman rules for the σ model: photon-nucleon, meson-nucleon, and meson-meson vertices.

vertex by

$$\frac{i}{q^2-\mu_1^2+i\epsilon}\frac{i}{(q+Q)^2-\mu_1^2+i\epsilon}$$

$$-\frac{i}{q^2-\Lambda^2+i\epsilon}\frac{i}{(q+Q)^2-\Lambda^2+i\epsilon}. \quad (54)$$

(iii) We use the finite, renormalized values for all of the superficially divergent nucleon loop diagrams illustrated in Fig. 12. These diagrams fall into six classes: (a) diagrams with external σ or π lines only, (b) diagrams with one axial-vector vertex and external meson lines, (c) diagrams with external photon lines only, (d) the axial-vector–photon–photon triangle diagram, (e) diagrams with external photon and meson lines, and (f) diagrams with an axial-vector vertex and external photon and meson lines. In Appendix A we give explicit renormalized expressions for the diagrams of types (a) and (b), and show that they satisfy the usual axial-vector Ward identities. The diagrams of type (c) (photon vacuum polarization loops) were considered in our discussion of spinor electrodynamics. The diagrams of types (d)–(f) are made finite and unique by calculating them in a gauge-invariant manner. As we have emphasized, the triangle diagram of type (d) does not satisfy the usual axial-vector Ward identity. We show in Appendix A that the axial-vector–photon–photon–meson box diagram [Fig. 12(f)] does satisfy the usual axial-vector Ward identity.

(iv) We take account of the counter term proportional to μ_0^2 in the following way. First, we omit *all* σ-meson tadpole diagrams (Fig. 9). (The recipe in Appendix A sets the basic nucleon loop tadpole equal to zero, but now tadpoles involving virtual meson integrations are to be dropped as well.) Second, when calculating pion self-energy diagrams $\Sigma^\pi(q^2)$ involving virtual meson integrations, a subtraction at $q=0$ should be performed to ensure that

$$\Sigma^\pi(0)=0. \quad (55)$$

[We will check explicitly below that the derivation of Eqs. (46)–(50) is valid in the cutoff theory.] This subtraction eliminates the formal quadratic divergence (which has become an actual logarithmic divergence in our cutoff theory) and leaves only formal logarithmic divergences, which are rendered finite by the cutoffs in the meson propagators. The σ self-energy is to be calculated from the pion self-energy by use of the equation

$$\Sigma^\sigma(q^2)=[\Sigma^\sigma(q^2)-\Sigma^\pi(0)]+\Sigma^\pi(0); \quad (56)$$

the quantity in square brackets is only formally logarithmically divergent, and hence finite in our cutoff theory. All other diagrams involving virtual meson integrations are automatically finite in the cutoff theory.

(v) There is a factor $\int d^4l/(2\pi)^4$ for each internal integration over loop variable l, a factor -1 for each fermion loop, a factor $\frac{1}{2}$ for each closed loop with one or two identical meson lines [Fig. 13(a)], and a factor $\frac{1}{6}$ for each closed loop with three identical meson lines [Fig. 13(b)].

(vi) We use the iterative renormalization procedure[10]

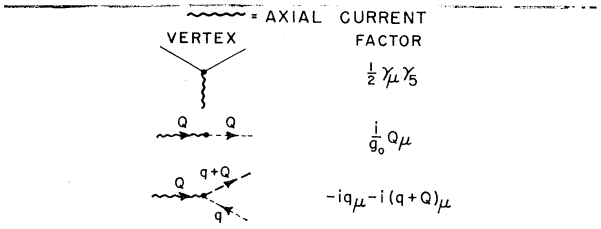

FIG. 11. Feynman rules for the σ model: axial-vector-current–nucleon and axial-vector-current–meson vertices.

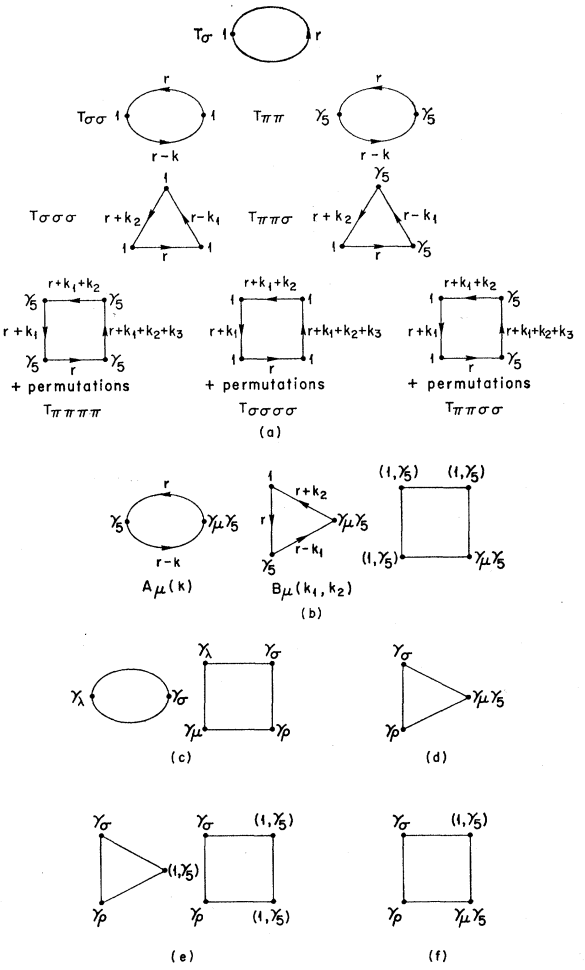

FIG. 12. Superficially divergent nucleon loop diagrams in the σ model. The six categories are described in the text immediately following Eq. (54).

[10] We make no attempt to *prove* renormalizability of the σ model. Renormalizability of the σ model (with only the mesons present) has recently been discussed by B. W. Lee, Nucl. Phys **B9**, 649 (1969), and renormalization of the closely related φ^4 meson theory has been analyzed by T. T. Wu, Phys. Rev. **125**, 1436 (1962).

to fix the unrenormalized quantities e_0, g_0, G_0, λ_0, $m_0=G_0/g_0$, μ_1, and the wave-function renormalizations Z_2 (fermion wave-function renormalization), Z_3^π, Z_3^σ, and $Z_3^\gamma=(e/e_0)^{1/2}$. For finite Λ, all of these will be *finite* functions of Λ and of the renormalized quantities e, g, G, λ, and μ, with μ the physical pion mass. (Alternatively, we can take the independent physical quantities to be e, m, G, λ, and μ, with m the physical nucleon mass.) We include wave-function renormalization factors $Z_2^{1/2}$, $(Z_3^\pi)^{1/2}$, $(Z_3^\sigma)^{1/2}$, and $(Z_3^\gamma)^{1/2}$ for each fermion pion, σ, and photon external line.

As in the case of spinor electrodynamics, the cutoff rules in the σ model are compactly summarized by the statement that they are the Feynman rules for the regulated Lagrangian density[11]:

$$\begin{aligned}\mathfrak{L}^R(x)=&\bar\psi[i\partial\!\!\!/-G_0(g_0^{-1}+\sigma^T+i\pi^T\gamma_5)]\psi+(D^{(2)}+\lambda_0)[4(\sigma^T)^2+4g_0\sigma^T((\sigma^T)^2+(\pi^T)^2)+g_0^2((\sigma^T)^2+(\pi^T)^2)^2]\\&+\tfrac{1}{2}E^{(2)}[(\partial\pi^T)^2+(\partial\sigma^T)^2]+\tfrac{1}{2}(F^{(2)}+\mu_0^2)[2g_0^{-1}\sigma^T+(\sigma^T)^2+(\pi^T)^2]+\tfrac{1}{2}[(\partial\pi)^2+(\partial\sigma)^2]-\tfrac{1}{2}\mu_1^2(\pi^2+\sigma^2)\\&-\tfrac{1}{2}[(\partial\pi^R)^2+(\partial\sigma^R)^2]+\tfrac{1}{2}\Lambda^2[(\pi^R)^2+(\sigma^R)^2]-\tfrac{1}{4}F_{\mu\nu}F^{\mu\nu}+\tfrac{1}{4}F_{\mu\nu}{}^RF^{R\mu\nu}-\tfrac{1}{2}\Lambda^2A_\mu{}^RA^{R\mu}-e_0\bar\psi\gamma_\mu\psi(A^\mu+A^{R\mu})\\&+C^{(2)}(F_{\mu\nu}+F_{\mu\nu}{}^R)(F^{\mu\nu}+F^{R\mu\nu}),\quad \pi^T=\pi+\pi^R,\quad \sigma^T=\sigma+\sigma^R. \qquad (57)\end{aligned}$$

The axial-vector current, generated by the gauge transformation

$$\begin{aligned}\psi&\longrightarrow(1+\tfrac{1}{2}i\gamma_5v)\psi,\\ \pi&\longrightarrow\pi-v(g_0^{-1}+\sigma),\\ g_0^{-1}+\sigma&\longrightarrow g_0^{-1}+\sigma+v\pi,\\ \pi^R&\longrightarrow\pi^R-v\sigma^R,\\ \sigma^R&\longrightarrow\sigma^R+v\pi^R,\end{aligned}\qquad (58)$$

is[12]

$$\begin{aligned}j_\mu{}^5=-\delta\mathfrak{L}^R/\delta(\partial^\mu v)=&\bar\psi\tfrac{1}{2}\gamma_\mu\gamma_5\psi+\sigma\partial_\mu\pi-\pi\partial_\mu\sigma+g_0^{-1}\partial_\mu\pi\\&-\sigma^R\partial_\mu\pi^R+\pi^R\partial_\mu\sigma^R+E^{(2)}\\&\times(\sigma^T\partial_\mu\pi^T-\pi^T\partial_\mu\sigma^T+g_0^{-1}\partial_\mu\pi^T). \qquad (59)\end{aligned}$$

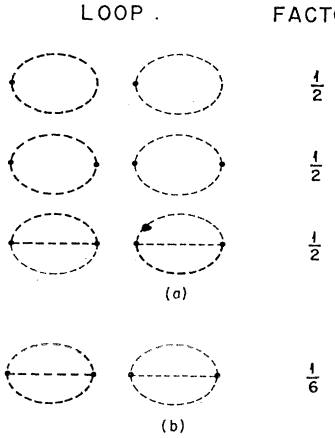

FIG. 13. Meson loop diagrams and corresponding Bose-symmetry factors.

[11] Since $\langle\sigma\rangle_0=\langle\sigma^R\rangle_0=0$, the conditions $\langle\delta\mathfrak{L}/\delta\sigma\rangle_0=\langle\delta\mathfrak{L}/\delta\sigma^R\rangle_0=0$ are identical.

[12] The modified Feynman rules for meson propagators attached to the axial-vector vertex [item (ii) above] follow directly from Eq. (59). The pion propagator immediately following the axial-vector-current–pion vertex is unregulated because $g_0^{-1}\partial_\mu\pi$ appears in Eq. (59) without an accompanying $g_0^{-1}\partial_\mu\pi^R$ term. Similarly, the *product* of meson propagators following the axial-vector-current–pion–σ vertex is regulated as in Eq. (54) because the bilinear terms in Eq. (59) have the difference-of-products form $\sigma\partial_\mu\pi-\pi\partial_\mu\sigma=(\sigma^R\partial_\mu\pi^R-\pi^R\partial_\mu\sigma^R)$.

The counter terms proportional to $D^{(2)}$, $E^{(2)}$, and $F^{(2)}$ perform the explicit subtractions in the loops illustrated in Figs. 12(a) and 12(b), just as $C^{(2)}$ provides the explicit subtraction in the basic vacuum polarization loop (see Appendix A for details).

We are now ready to calculate the divergence of the axial-vector current in our cutoff theory. One way to do this is to proceed diagrammatically, as we did in Eqs. (10)–(14) in the spinor electrodynamics case. However, because of the complexity of the σ model, this method will involve very complicated equations. Therefore, we will instead follow the second, more succinct, method used in spinor electrodynamics. We note first that calculation of the axial-vector divergence in the regulated σ model by naive use of the equations of motion gives

$$\partial^\mu j_\mu{}^5=-\delta\mathfrak{L}^R/\delta v=-(\mu_1{}^2/g_0)\pi. \qquad (60)$$

Extra terms on the right-hand side of Eq. (60) can arise only from diagrams which are so singular that the Ward identities break down. However, since we have cut off the photon and meson propagators, all virtual boson integrations are strongly convergent and cannot lead to singularities which are not present when the boson integrations are omitted. Thus, breakdown of Eq. (60) can only be associated with the basic axial-vector loops shown in Figs. 12(b), 12(d), and 12(f). (All other axial-vector loops have enough vertices, and hence are convergent enough, to satisfy the normal axial-vector Ward identities.) By explicit calculation, we have found that of these diagrams, only the axial-vector–vector–vector triangle of Fig. 12(d) has an anomalous Ward identity, leading to the conclusion that, in the regulated σ model, the axial-vector-current divergence equation is

$$\begin{aligned}\partial^\mu j_\mu{}^5=&-(\mu_1{}^2/g_0)\pi+\tfrac{1}{2}(\alpha_0/4\pi)(F^{\xi\sigma}+F^{R\xi\sigma})\\&\times(F^{\tau\rho}+F^{R\tau\rho})\epsilon_{\xi\sigma\tau\rho}. \qquad (61)\end{aligned}$$

This completes our verification that Eq. (4) is exact to all orders of the strong and electromagnetic couplings in the σ model.

From Eq. (61) a number of consequences immediately follow.

(i) We can check the consistency of our cutoff Feynman rules by verifying that Eq. (55) is really valid in the regulated theory. As in Eq. (46), we define

$$\Delta_F^{\pi\prime}(q)=-i\int d^4x\, e^{iq\cdot x}\langle T(\pi(x)\pi(0))\rangle_0, \qquad (62)$$

and substitute Eq. (61) for $\pi(x)$. Using Eq. (59) for $j_\mu^5(x)$, and the canonical commutation relation

$$[\partial^0\pi(x)+E^{(2)}\partial^0\pi^T(x),\pi(0)]|_{x_0=0}=-i\delta^3(\mathbf{x}), \qquad (63)$$

we still find the result $\Delta_F^{\pi\prime}(0)=-1/\mu_1^2$. The relation between $\Delta_F^{\pi\prime}(q)$ and the proper pion self-energy $\Sigma^\pi(q^2)$ in the cutoff theory is given by

$$\Delta_F^{\pi\prime}(q)=\frac{1}{q^2-\mu_1^2}+\frac{1}{q^2-\mu_1^2}\Sigma^\pi(q^2)\frac{1}{q^2-\mu_1^2}+\frac{1}{q^2-\mu_1^2}\Sigma^\pi(q^2)\left(\frac{1}{q^2-\mu_1^2}-\frac{1}{q^2-\Lambda^2}\right)\Sigma^\pi(q^2)\frac{1}{q^2-\mu_1^2}$$
$$+\frac{1}{q^2-\mu_1^2}\Sigma^\pi(q^2)\left(\frac{1}{q^2-\mu_1^2}-\frac{1}{q^2-\Lambda^2}\right)\Sigma^\pi(q^2)\left(\frac{1}{q^2-\mu_1^2}-\frac{1}{q^2-\Lambda^2}\right)\Sigma^\pi(q^2)\frac{1}{q^2-\mu_1^2}+\cdots$$
$$=\frac{1+\Sigma^\pi(q^2)(q^2-\Lambda^2)^{-1}}{q^2-\mu_1^2+\Sigma^\pi(q^2)(\mu_1^2-\Lambda^2)(q^2-\Lambda^2)^{-1}}, \qquad (64)$$

so that

$$\Delta_F^{\pi\prime}(0)=\frac{1-\Sigma^\pi(0)\Lambda^{-2}}{-\mu_1^2-\Sigma^\pi(0)(\mu_1^2-\Lambda^2)\Lambda^{-2}}, \qquad (65)$$

and therefore Eq. (49) still implies that $\Sigma^\pi(0)=0$.

(ii) In the absence of electromagnetism, Eq. (61) becomes the usual PCAC equation $\partial^\mu j_\mu^5=-(\mu_1^2/g_0)\pi$. From this equation, it is straightforward to prove[13] that the coupling-constant, mass, and wave-function renormalizations which make S-matrix elements in the σ model finite also make all matrix elements of j_μ^5 and of $(\mu_1^2/g_0)\pi$ finite (i.e., cutoff-independent as $\Lambda\to\infty$). In the presence of electromagnetism, the effect of the extra term in Eq. (61), as shown in I, is to induce an extra infinity in j_μ^5 which is *not* removed by the renormalizations which make the S matrix finite. However, just as we found that $m_0 j^5(x)$ is made finite by the fermion wave-function renormalization in spinor electrodynamics, we expect that, even in the presence of electromagnetism, $(\mu_1^2/g_0)\pi$ will be made finite by the pion wave-function renormalization in the σ model. That is, we expect

$$(\mu_1^2/g_0)(Z_3^\pi)^{1/2}=\text{finite}. \qquad (66)$$

Since the pion field is multiplicatively renormalizable,

$$\pi=(Z_3^\pi)^{1/2}\pi^{\text{renorm}}, \qquad (67)$$

to prove Eq. (66) we only need show that any particular nonvanishing matrix element of $(\mu_1^2/g_0)\pi$ is finite. The natural choice is the vacuum to two-photon matrix element $G^\pi(k_1\cdot k_2)$, defined by

$$\langle\gamma(k_1,\epsilon_1)\gamma(k_2,\epsilon_2)|(-\mu_1^2/g_0)\pi|0\rangle$$
$$=(4k_{10}k_{20})^{-1/2}k_1^\xi k_2^\tau\epsilon_1^{*\sigma}\epsilon_2^{*\rho}\epsilon_{\xi\tau\sigma\rho}G^\pi(k_1\cdot k_2). \qquad (68)$$

Precisely the same arguments leading to Eq. (23) show that

$$G^\pi(0)=-\alpha/\pi, \qquad (69)$$

proving Eq. (66). We are now free to let the cutoff Λ approach infinity, defining a renormalized matrix element $\tilde{G}^\pi(k_1\cdot k_2)$,

$$\lim_{\Lambda\to\infty}G^\pi(k_1\cdot k_2)=\tilde{G}^\pi(k_1\cdot k_2), \qquad (70)$$

which satisfies the exact low-energy theorem

$$\tilde{G}^\pi(0)=-\alpha/\pi. \qquad (71)$$

In Sec. III, we will explicitly check Eq. (71) to second order in the strong meson-nucleon coupling constant G.

(iii) The low-energy theorem of Eq. (71) can be rewritten in a physically interesting form, as follows. We introduce the $\pi\to 2\gamma$ decay amplitude $F^\pi(k_1\cdot k_2)$ and the pion weak decay amplitude f_π by writing

$$\langle\gamma(k_1,\epsilon_1)\gamma(k_2,\epsilon_2)|(\Box^2+\mu^2)\pi^{\text{renorm}}|0\rangle$$
$$=(4k_{10}k_{20})^{-1/2}k_1^\xi k_2^\tau\epsilon_1^{*\sigma}\epsilon_2^{*\rho}\epsilon_{\xi\tau\sigma\rho}F^\pi(k_1\cdot k_2), \qquad (72)$$

and

$$\langle\pi(q)|j_\mu^5|0\rangle=(2q_0)^{-1/2}(-iq_\mu/\mu^2)f_\pi/\sqrt{2}. \qquad (73)$$

Comparing Eq. (72) with Eqs. (68) and (71), we find

$$\frac{-\mu_1^2}{g_0}\frac{(Z_3^\pi)^{1/2}}{\mu^2}F^\pi(0)=\frac{-\alpha}{\pi}, \qquad (74)$$

while taking the divergence of Eq. (73) and using Eq. (61) gives

$$f_\pi/\sqrt{2}=(-\mu_1^2/g_0)(Z_3^\pi)^{1/2}$$
$$+(\text{terms of higher order in }\alpha). \qquad (75)$$

Combining Eqs. (74) and (75) then gives the low-energy theorem relating the $\pi\to 2\gamma$ and π weak decay ampli-

[13] J. Bernstein, M. Gell-Mann, and L. Michel, Nuovo Cimento **16**, 560 (1960); Preparata and Weisberger (Ref. 9).

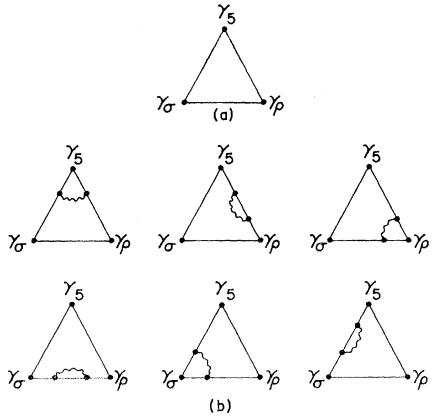

FIG. 14. (a) γ_5-γ_σ-γ_ρ skeleton triangle. (b) Second-order radiative corrections to the γ_5-γ_σ-γ_ρ triangle in spinor electrodynamics.

tudes,

$$F^\pi(0)=(-\alpha/\pi)(\sqrt{2}\mu^2/f_\pi) + (\text{terms of higher order in } \alpha). \quad (76)$$

The fact that Eq. (61) is exact means that Eq. (76) is true to all orders in the strong interactions in the σ model. The experimental consequences of Eq. (76) are discussed in I.

III. SECOND-ORDER CALCULATION

We give in this section an explicit second-order calculation to check our contention that Eqs. (2) and (4) are exact. Rather than calculating corrections to both the axial-vector and pseudoscalar or pion vertices and checking Eqs. (2) and (4) directly, we will check these equations *indirectly* by verifying the low-energy theorems (30) and (71) which they imply. In the case of spinor electrodynamics, we will calculate the second-order radiative corrections to the matrix element $\langle\gamma(k_1,\epsilon_1)\gamma(k_2,\epsilon_2)|2im_0\bar{\psi}\gamma_5\psi|0\rangle$, which arise from the six diagrams shown in Fig. 14(b). These diagrams [plus mass counter terms appearing in the basic γ_5-γ_σ-γ_ρ triangle of Fig. 14(a)] make a contribution to $\tilde{G}(0)$ of order α^2, which must, in fact, be zero for Eq. (30) to be correct. The vanishing of the α^2 term is clearly a test of the absence of a term proportional to $\alpha\alpha_0 F^{\xi\sigma}F^{\tau\rho}\epsilon_{\xi\sigma\tau\rho}$ in Eq. (2).

Similarly, in the σ model we will calculate radiative corrections to $\langle\gamma(k_1,\epsilon_1)\gamma(k_2,\epsilon_2)|(-\mu_1{}^2/g_0)\pi|0\rangle$. It is convenient to rewrite this matrix element by substituting for $\mu_1{}^2\pi$ the pion equation of motion obtained from Eq. (31),

$$\mu_1{}^2\pi=-\Box^2\pi-iG_0\bar{\psi}\gamma_5\psi + \lambda_0[8g_0\sigma\pi+4g_0{}^2\pi(\sigma^2+\pi^2)]+\mu_0{}^2\pi. \quad (77)$$

The matrix element of $\Box^2\pi$ makes a contribution to $\tilde{G}^\pi(k_1\cdot k_2)$ of order $k_1\cdot k_2$, and thus can be neglected at $k_1\cdot k_2=0$. If we work to second order in G^2 but to zeroth order in λ, so that the physical pion and σ masses remain equal, the meson-meson scattering terms in Eq. (77) can also be dropped. Finally, let us recall that the effect of the counter term proportional to $\mu_0{}^2$ is to produce a subtraction in the pion proper self-energy, giving $\Sigma^\pi(0)=0$. In particular, this means that the counter term $\mu_0{}^2\pi$ in Eq. (77) combines with the nucleon bubble diagram involving $-iG_0\bar{\psi}\gamma_5\psi$, shown in Fig. 15, to give a contribution to $\tilde{G}^\pi(k_1\cdot k_2)$ proportional to $\Sigma^\pi(2k_1\cdot k_2)$, which vanishes at $k_1\cdot k_2=0$. Recalling that $G_0/g_0=m_0$, we may summarize the findings of this paragraph by the statement that to check the low-energy theorem of Eq. (71) to order G^2, we need only calculate the matrix element $\langle\gamma(k_1,\epsilon_1)\gamma(k_2,\epsilon_2)|im_0\bar{\psi}\gamma_5\psi|0\rangle$, omitting the bubble diagram of Fig. 15. The twelve diagrams which contribute have the form of those in Fig. 14(b), with the virtual photon line replaced by a virtual pion or a virtual σ line. These diagrams, plus mass counter terms in the basic triangle of Fig. 14(a), make a contribution to $\tilde{G}^\pi(0)$ of order $G^2\alpha$, which must vanish for Eq. (71) to be valid [thereby verifying the absence of a term proportional to $G^2\alpha_0 F^{\xi\sigma}F^{\tau\rho}\epsilon_{\xi\sigma\tau\rho}$ in Eq. (14)]. Thus we see that the second-order spinor electrodynamics and σ-model calculations will appear very similar.

The calculations of the second-order radiative corrections to the triangle diagram will proceed in the following way. First, we calculate the renormalized quantities $\tilde{\Gamma}_\mu(p,p')$, $\tilde{\Gamma}^5(p,p')$, and $\tilde{S}_F'(p)$ in spinor electrodynamics and the σ model, and substitute them into the γ_5-γ_σ-γ_ρ skeleton triangle of Fig. 14(a). The constants $\tilde{G}(0)$ and $\tilde{G}^\pi(0)$ are determined by extracting the first nonvanishing terms of a Taylor series expansion of the amplitudes in the photon momenta k_1 and k_2. The Ward identities and integrations by parts are used to show that the self-energy corrections are exactly canceled by the unexpanded vertex corrections. The terms where an external momentum has been expanded from a vertex correction function are evaluated in two ways: by direct calculation and by using a further integration by parts. Using either method, the sum of these terms is found to vanish. Therefore, the second-order radiative corrections to $\tilde{G}(0)$ and $\tilde{G}^\pi(0)$ are zero.

Let $\tilde{\Gamma}_\mu{}^{(2)}(p,p')$, $\tilde{\Gamma}_5{}^{(2)}(p,p')$, and $\tilde{S}_F'{}^{(2)}(p)$ denote the renormalized second-order vector vertex, pseudoscalar vertex, and fermion propagator in either spinor electrodynamics or the σ model, as defined by Eqs. (25) and (28). (Explicit expressions for these quantities are given in Appendix B.) The matrix element which we want

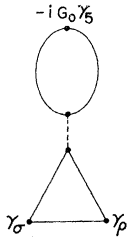

FIG. 15. Nucleon bubble diagram, which in the σ model appears in the second-order radiative corrections to the γ_5-γ_σ-γ_ρ triangle.

is proportional to

$$\mathfrak{M}_{\sigma\rho}=\int d^4r\ \mathrm{Tr}[\tilde{\Gamma}_5^{(2)}(r-k_2,r+k_1)\tilde{S}_F'^{(2)}(r+k_1)\times\tilde{\Gamma}_\sigma^{(2)}(r+k_1,r)\tilde{S}_F'^{(2)}(r)\tilde{\Gamma}_\rho^{(2)}(r,r-k_2)\times\tilde{S}_F'^{(2)}(r-k_2)]. \quad (78)$$

Since we are actually only interested in studying the part of Eq. (78) coming from the second-order radiative corrections, let us substitute

$$\begin{aligned}\tilde{\Gamma}_\mu^{(2)}(p,p')&=\gamma_\mu+\Lambda_\mu(p,p'),\\ \tilde{\Gamma}_5^{(2)}(p,p')&=\gamma_5+\Lambda_5(p,p'),\\ \tilde{S}_F'^{(2)}(p)&=[\not{p}-m-\Sigma(\not{p})]^{-1}\end{aligned} \quad (79)$$

into Eq. (78) and isolate the second-order part. This gives

$$\mathfrak{M}_{\sigma\rho}{}^{(2)}=\int d^4r\ \mathrm{Tr}[\Lambda_5(r-k_2,r+k_1)(\not{r}+\not{k}_1-m)^{-1}\gamma_\sigma(\not{r}-m)^{-1}\gamma_\rho(\not{r}-\not{k}_2-m)^{-1} \quad (80a)$$

$$+\gamma_5(\not{r}+\not{k}_1-m)^{-1}\Sigma(\not{r}+\not{k}_1)(\not{r}+\not{k}_1-m)^{-1}\gamma_\sigma(\not{r}-m)^{-1}\gamma_\rho(\not{r}-\not{k}_2-m)^{-1} \quad (80b)$$

$$+\gamma_5(\not{r}+\not{k}_1-m)^{-1}\Lambda_\sigma(r+k_1,r)(\not{r}-m)^{-1}\gamma_\rho(\not{r}-\not{k}_2-m)^{-1} \quad (80c)$$

$$+\gamma_5(\not{r}+\not{k}_1-m)^{-1}\gamma_\sigma(\not{r}-m)^{-1}\Sigma(\not{r})(\not{r}-m)^{-1}\gamma_\rho(\not{r}-\not{k}_2-m)^{-1} \quad (80d)$$

$$+\gamma_5(\not{r}+\not{k}_1-m)^{-1}\gamma_\sigma(\not{r}-m)^{-1}\Lambda_\rho(r,r-k_2)(\not{r}-\not{k}_2-m)^{-1} \quad (80e)$$

$$+\gamma_5(\not{r}+\not{k}_1-m)^{-1}\gamma_\sigma(\not{r}-m)^{-1}\gamma_\rho(\not{r}-\not{k}_2-m)^{-1}\Sigma(\not{r}-\not{k}_2)(\not{r}-\not{k}_2-m)^{-1}], \quad (80f)$$

with the six terms in Eq. (80) corresponding, of course, to the six diagrams in Fig. 14(b). To evaluate Eq. (80), we use the fact that although the integral over r is apparently linearly divergent, the linearly divergent parts of terms (80a)–(80f) vanish separately when the trace is taken.[14] This means that we can simplify the form of Eq. (80) by making separate translations of the integration variable in each of the pieces (80a)–(80f), as follows:

(a) $r\to r+k_2$, (d) $r\to r$,
(b) $r\to r-k_1$, (e) $r\to r$,
(c) $r\to r-k_1$, (f) $r\to r+k_2$.

After making these translations, wherever Σ appears it has argument r, and the vertex parts Λ_5, Λ_σ, and Λ_ρ have r as the first argument. Next, we Taylor-expand with respect to k_1 and k_2, keeping only the leading term of order k_1k_2 (because of the γ_5, the terms of order 1, k_1, k_2, k_1^2, and k_2^2 vanish identically). Defining the vertex derivatives $\Lambda_{5,\xi}(r)$ and $\Lambda_{\sigma,\xi}(r)$ by

$$\begin{aligned}\Lambda_5(r,r+a)&=\Lambda_5(r,r)+a^\xi\Lambda_{5,\xi}(r)+O(a^2),\\ \Lambda_\sigma(r,r+a)&=\Lambda_\sigma(r,r)+a^\xi\Lambda_{\sigma,\xi}(r)+O(a^2),\end{aligned} \quad (81)$$

we find

$$\mathfrak{M}_{\sigma\rho}{}^{(2)}=\mathfrak{M}_{A\sigma\rho}{}^{(2)}+\mathfrak{M}_{B\sigma\rho}{}^{(2)}+(\text{terms of higher order in momenta}), \quad (82)$$

with [we abbreviate $s\equiv(\not{r}-m)^{-1}$]

$$\mathfrak{M}_{A\sigma\rho}{}^{(2)}\equiv k_1{}^\xi k_2{}^\tau\mathfrak{M}_{A\xi\tau\sigma\rho}{}^{(2)}$$

$$=\int d^4r\ \mathrm{Tr}[\Lambda_5(r,r)s(-\not{k}_1)s\gamma_\sigma s(-\not{k}_2)s\gamma_\rho s+\gamma_5 s\Sigma(\not{r})s\gamma_\sigma s\not{k}_1 s\gamma_\rho s\not{k}_2 s+\gamma_5 s\Lambda_\sigma(r,r)s\not{k}_1 s\gamma_\rho s\not{k}_2 s$$
$$+\gamma_5 s(-\not{k}_1)s\gamma_\sigma s\Sigma(\not{r})s\gamma_\rho s\not{k}_2 s+\gamma_5 s(-\not{k}_1)s\gamma_\sigma s\Lambda_\rho(r,r)s\not{k}_2 s+\gamma_5 s(-\not{k}_1)s\gamma_\sigma s(-\not{k}_2)s\gamma_\rho s\Sigma(\not{r})s], \quad (83)$$

and with

$$\mathfrak{M}_{B\sigma\rho}{}^{(2)}\equiv k_1{}^\xi k_2{}^\tau\mathfrak{M}_{B\xi\tau\sigma\rho}{}^{(2)}$$

$$=\int d^4r\ \mathrm{Tr}[k_1{}^\xi\Lambda_{5,\xi}(r)s\gamma_\sigma s(-\not{k}_2)s\gamma_\rho s+\gamma_5 s(-k_1{}^\xi)\Lambda_{\sigma,\xi}(r)s\gamma_\rho s\not{k}_2 s+\gamma_5 s(-\not{k}_1)s\gamma_\sigma s(-k_2{}^\tau)\Lambda_{\rho,\tau}(r)s]. \quad (84)$$

The tensors $\mathfrak{M}_{A\xi\tau\sigma\rho}{}^{(2)}$ and $\mathfrak{M}_{B\xi\tau\sigma\rho}{}^{(2)}$ must both have the structure

$$\begin{aligned}\mathfrak{M}_{A\xi\tau\sigma\rho}{}^{(2)}&=\epsilon_{\xi\tau\sigma\rho}\mathfrak{M}_A{}^{(2)},\\ \mathfrak{M}_{B\xi\tau\sigma\rho}{}^{(2)}&=\epsilon_{\xi\tau\sigma\rho}\mathfrak{M}_B{}^{(2)},\end{aligned} \quad (85)$$

and therefore are completely antisymmetric in their indices. Clearly, each *individual term* in the sums in Eqs. (83) and (84) will also have the form of Eq. (85),

[14] Simple γ-matrix counting shows that trace of each of the terms (80a)–(80f) is proportional to the fermion mass m, and is therefore, on dimensional grounds, at most logarithmically divergent. Because of the over-all factor γ_5, the logarithmic divergences vanish as well, so that the integrals of terms (80a)–(80f) actually converge.

once the integration over r is performed. This fact greatly simplifies the following calculation.

To evaluate $\mathfrak{M}_{A\xi\tau\sigma\rho}{}^{(2)}$, we eliminate the vertex parts from Eq. (83) by using the Ward identities

$$\begin{aligned}\Lambda_5(r,r)&=(1/2m)[\gamma_5\Sigma(r)+\Sigma(r)\gamma_5],\\ \Lambda_\lambda(r,r)&=-\partial_\lambda\Sigma(r),\\ -\partial_\lambda(r-m)^{-1}&=(r-m)^{-1}\gamma_\lambda(r-m)^{-1}.\end{aligned}\tag{86}$$

Integration by parts in the terms involving $\partial_\lambda\Sigma(r)$ shifts the derivatives to the free propagators $(r-m)^{-1}$. The resultant amplitudes all involve a trace containing γ matrices, r, and $\Sigma(r)$. By anticommuting r through the γ matrices and using the total antisymmetry of $\mathfrak{M}_{A\xi\tau\sigma\rho}{}^{(2)}$ in its tensor indices, we find

$$\begin{aligned}\mathfrak{M}_{A\xi\tau\sigma\rho}{}^{(2)}=\int d^4r\,\{&(r^2-m^2)^{-3}\\ &\times\mathrm{Tr}[\tfrac{1}{2}(\gamma_5\Sigma(r)+\Sigma(r)\gamma_5)\gamma_\xi\gamma_\sigma\gamma_\tau\gamma_\rho]\\ &+(r^2-m^2)^{-4}\,\mathrm{Tr}[(r+m)\Sigma(r)(r+m)\gamma_5\gamma_\xi\gamma_\sigma\gamma_\tau\gamma_\rho]\\ &-(r^2-m^2)^{-4}8r_\sigma\,\mathrm{Tr}[\Sigma(r)(r+m)\gamma_5\gamma_\xi\gamma_\tau\gamma_\rho]\}.\end{aligned}\tag{87}$$

On substitution of the general expression $\Sigma(r)=A(r^2)+rB(r^2)$ and use of symmetric integration in r, we find that the right-hand side of Eq. (87) vanishes, implying $\mathfrak{M}_{A\xi\tau\sigma\rho}{}^{(2)}=0$.

The evaluation of $\mathfrak{M}_{B\xi\tau\sigma\rho}{}^{(2)}$ in Eq. (84) will be done using two different methods, each giving zero. The first method involves a direct calculation of the integrals. We recall that each term of Eq. (84) is totally antisymmetric in the tensor indices, once the integration over r is performed. Using this total antisymmetry and reversing the order of the γ matrix products in the third term in Eq. (84) yields

$$\begin{aligned}\mathfrak{M}_{B\xi\tau\sigma\rho}{}^{(2)}=\int d^4r\,\mathrm{Tr}\{&\Lambda_{5,\xi}(r)s\gamma_\sigma s(-\gamma_\tau)s\gamma_\rho s\\ &+\gamma_5 s[-\Lambda_{\sigma,\xi}(r)+\Lambda_{\sigma,\xi}(r)^R]s\gamma_\rho s\gamma_\tau s\},\end{aligned}\tag{88}$$

where $\Lambda_{\sigma,\xi}{}^{(2)}(r)^R$ is obtained from $\Lambda_{\sigma,\xi}{}^{(2)}(r)$ by reversing the order of all γ-matrix products. From Appendix B, we find the expressions

$$\begin{aligned}\Lambda_{5,\xi}(r)&=\gamma_5\gamma_\xi E_1(r^2)+\gamma_5 r_\xi E_2(r^2),\\ \Lambda_{\sigma,\xi}(r)&=\gamma_\sigma r_\xi D_1(r^2)+\gamma_\xi\gamma_\sigma r D_2(r^2)+r\gamma_\sigma\gamma_\xi D_3(r^2)\\ &\quad+g_{\sigma\xi}D_4(r^2)+r_\sigma r_\xi D_5(r^2)+r_\sigma r_\xi r D_6(r^2),\\ \Lambda_{\sigma,\xi}(r)^R&=\gamma_\sigma r_\xi D_1(r^2)+r\gamma_\sigma\gamma_\xi D_2(r^2)+\gamma_\xi\gamma_\sigma r D_3(r^2)\\ &\quad+g_{\sigma\xi}D_4(r^2)+r_\sigma r_\xi D_5(r^2)+r_\sigma r_\xi r D_6(r^2),\end{aligned}\tag{89}$$

where E_1, E_2, $D_1,\cdots$, are simple integrals over Feynman parameters. Substituting Eq. (89) into Eq. (88) and evaluating the trace gives

$$\begin{aligned}\mathfrak{M}_B{}^{(2)}=-4i\int d^4r\,\{&m^2E_1(r^2)\\ &-mr^2[D_2(r^2)-D_3(r^2)]\}(r^2-m^2)^{-3}.\end{aligned}\tag{90}$$

From Appendix B we find

$$\begin{aligned}E_1(r^2)&=\frac{1}{16\pi^2}\begin{Bmatrix}e^2\\-G^2\end{Bmatrix}\\ &\quad\times\int_0^1 zdz\,\frac{-2m}{-r^2z(1-z)+zm^2+(1-z)\mu^2},\\ D_2(r^2)-D_3(r^2)&=\frac{1}{16\pi^2}\begin{Bmatrix}e^2\\-G^2\end{Bmatrix}\\ &\quad\times\int_0^1 zdz\,\frac{2(1-z)}{-r^2z(1-z)+zm^2+(1-z)\mu^2},\end{aligned}\tag{91}$$

where the upper (lower) entry in { } refers to spinor electrodynamics (the σ model), and where μ^2 is the virtual photon, pion, or σ mass. Inserting Eq. (91) into Eq. (90), we find that the integral in Eq. (90) is proportional to $I(\mu^2/m^2)$, with

$$I(a)\equiv\int_0^1 zdz\int_0^\infty\frac{udu}{(u+1)^3}\,\frac{1-u(1-z)}{uz(1-z)+z+(1-z)a}.\tag{92}$$

We show in Appendix C that this integral is identically zero, giving $\mathfrak{M}_B{}^{(2)}=0$.

The second method used to evaluate $\mathfrak{M}_{B\xi\tau\sigma\rho}{}^{(2)}$ involves the use of an integration by parts. Since the derivative on the vertex function removes the effect of the renormalization constants, the three terms in Eq. (84) may be written diagrammatically as shown in Fig. 16(a). In the first term in Eq. (84), we use Eq. (86) to replace $(r-m)^{-1}\gamma_\rho(r-m)^{-1}$ by $-\partial_\rho(r-m)^{-1}$, and then integrate by parts, using the total antisymmetry of the amplitude to drop the terms in which the derivative acts on the propagators adjacent to k_1 and γ_σ. This operation has the effect of replacing the left-hand diagram in Fig. 16(a) by the diagram in Fig. 16(b). The expression for $\mathfrak{M}_{B\xi\tau\sigma\rho}{}^{(2)}$ becomes

$$\begin{aligned}\mathfrak{M}_{B\sigma\rho}{}^{(2)}&=k_1{}^\xi k_2{}^\tau\mathfrak{M}_{B\xi\tau\sigma\rho}{}^{(2)}\\ &=\int d^4r\,\mathrm{Tr}[\gamma_5 s(-k_1)sk_2{}^\tau\Lambda_{\sigma,\tau}(r)s(-\gamma_\rho)s\\ &\quad+\gamma_5 s(-k_1{}^\xi)\Lambda_{\sigma,\xi}(r)s\gamma_\rho sk_2 s\\ &\quad+\gamma_5 s(-k_1)s\gamma_\sigma s(-k_2{}^\tau)\Lambda_{\rho,\tau}(r)s].\end{aligned}\tag{93}$$

Each term in the sum of Eq. (95) involves a trace containing γ matrices, r, and the function $\Lambda_{\sigma,\xi}(r)$. By anticommuting r through the γ matrices and by using

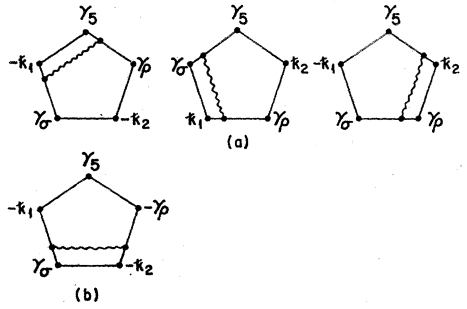

FIG. 16. (a) Diagrammatic representation of $\mathfrak{M}_{B\sigma\rho}^{(2)}$ in spinor electrodynamics. (b) Diagram obtained from the left-hand loop in (a) by integration by parts.

the antisymmetry of $\mathfrak{M}_{B\xi\tau\sigma\rho}^{(2)}$ in its indices, one finds

$$\mathfrak{M}_{B\xi\tau\sigma\rho}^{(2)}=\int d^4r\,(r^2-m^2)^{-2}\,\mathrm{Tr}\{\gamma_5\Lambda_{\sigma,\rho}(r)\tfrac{1}{2}[\gamma_\xi,\gamma_\tau]\}\,. \quad (94)$$

(The terms coming from the anticommutators exactly cancel because of the antisymmetry.) Substituting Eq. (89) into Eq. (94) immediately gives $\mathfrak{M}_{B\xi\tau\sigma\rho}^{(2)}=0$. It is not actually necessary to have the detailed form of Eq. (89) to see that Eq. (94) vanishes. Referring to Fig. 17(a), we see that in spinor electrodynamics $\Lambda_{\sigma,\rho}$ has the form

$$\Lambda_{\sigma,\rho}=\gamma_\alpha\Lambda_{\sigma,\rho}'(r)\gamma^\alpha, \quad (95)$$

and when Eq. (95) is substituted into Eq. (94), the sum over virtual photon polarization states α cancels to zero. Similarly, from Fig. 17(b) we see that in the σ model $\Lambda_{\sigma,\rho}$ has the property[15]

$$\Lambda_{\sigma,\rho}(r)=i\gamma_5\Lambda_{\sigma,\rho}(r)i\gamma_5, \quad (96)$$

which again implies that Eq. (94) vanishes. In this case, the virtual pion term is exactly canceled by the virtual σ term.

IV. SUMMARY AND DISCUSSION

We summarize our results and briefly compare them with the recent findings of Jackiw and Johnson.[2] We have considered two models, spinor electrodynamics and a truncated version of the σ model. In each model, we have studied a *particular* axial-vector current: in spinor electrodynamics, the usual axial-vector current of Eq. (1), and in the σ model, the Polkinghorne[16] axial-vector current of Eq. (3), which, in the absence of electromagnetism, obeys the PCAC condition. By introducing cutoffs in the boson propagators we have shown that, in the presence of electromagnetism, the divergences of our axial-vector currents are modified in a simple well-defined way, to *all* orders of perturbation theory. The modification consists of the addition of a simple numerical mutliple of $(\alpha_0/4\pi)F^{\xi\sigma}F^{\tau\rho}\epsilon_{\xi\sigma\tau\rho}$ to the naive axial-vector divergence. (The naive divergence is the one obtained by formal manipulation of equations of motion when subtleties arising from the singularity of local-field products are neglected.) From the anomalous divergence equations we obtained simple low-energy theorems for the vacuum-to-2γ matrix element of the naive divergence. Although these theorems were derived with the cutoff Λ finite, we argued that in both models, even in the presence of electromagnetism, the naive divergence is a finite (cutoff-independent) operator as $\Lambda\to\infty$.[17] This allowed us to pass freely to the limit $\Lambda\to\infty$, obtaining a low-energy theorem for the renormalized naive divergence operator. This low-energy theorem was checked explicitly to second order in radiative corrections in a calculation using only renormalized (cutoff-independent) quantities, verifying our contention that no subtleties were involved in the $\Lambda\to\infty$ limit.

Thus, in our calculation, use of the cutoff has been an artifice, and the cutoff does not appear in the physics. As is made clear by the discussion of Eqs. (66)–(70), this important feature can be traced directly back to the following property of the two axial-vector currents which we have studied: *The naive divergences of the two axial-vector currents, as well as the axial-vector currents themselves, are multiplicatively renormalizable.* We conjecture that in any renormalizable theory field with an axial-vector current satisfying this property, arguments analogous to those of this paper can be carried through.

With these comments in mind, let us examine the conclusions of Jackiw and Johnson. Jackiw and Johnson treat the electromagnetic field as an external (nonquantized) variable, but allow quantized strong interactions of the spinor particles, so their calculation applies, for example, to the σ model. Rather than considering the Polkinghorne current of Eq. (3), Jackiw and Johnson take as the axial-vector current the fermion part $\bar\psi\gamma_\mu\gamma_5\psi$ alone. They find that the effect of the strong interactions on the anomalous divergence term is ambiguous, and depends on precisely how a cutoff is introduced. It is easy to see that (even in the absence of electromagnetism) the current $\bar\psi\gamma_\mu\gamma_5\psi$ is *not* made finite by the usual renormalizations which make

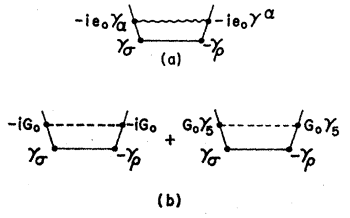

FIG. 17. Diagrammatic representation of $\Lambda_{\sigma,\rho}$ in (a) spinor electrodynamics and (b) the σ model.

[15] Comparing Eq. (96) with Eq. (89), we see that in the σ model, we must have $D_4=D_5=0$. This can be verified from the explicit formulas of Appendix B.

[16] J. C. Polkinghorne, Nuovo Cimento 8, 179 (1958); 8, 781 (1958).

[17] That is, multiplication by the usual external-line wave-function renormalization factors makes Feynman amplitudes of the naive divergence finite.

the S matrix in the σ model finite, and, by a reversal of the Preparata-Weisberger argument,[18] this means that the naive divergence of this current is *not* multiplicatively renormalizable. In other words, the axial-vector current considered by Jackiw and Johnson and its naive divergence are not well-defined objects in the usual renormalized perturbation theory; hence the ambiguous results which these authors have obtained are not too surprising.

The presence of two different axial-vector currents in the σ model poses, however, the following question: Which current should we take as the prototype for the *physical* axial-vector current? The answer is that there are two arguments in favor of using the full Polkinghorne current, rather than its fermion part alone, as the current to which the semileptonic weak interactions couple: (i) We want the physical axial-vector current to satisfy the PCAC hypothesis. Although PCAC does not require that the divergence of the axial-vector current be a canonical pion field (as is the case for the Polkinghorne current), it does require that it at least be a *smooth* interpolating field for the pion. However, a non-multiplicatively renormalizable operator, such as the divergence of the current $\bar{\psi}\gamma_\mu\gamma_5\psi$, will *not* be a smooth operator and therefore is not a pion interpolating field suitable for PCAC arguments. (ii) When charged fields and charged currents are added to the model, we want the axial-vector currents to satisfy the Gell-Mann current-algebra hypothesis. As Gell-Mann and Lévy[3] have shown, the Polkinghorne axial-vector current is the one which obeys the current algebra. The fermion part alone does not satisfy the current algebra.

To summarize, then, in the σ model (and also in the neutral-vector-meson model, which behaves like spinor electrodynamics), the current which is a prototype for the physical axial-vector current has a simple anomalous divergence term in the presence of electromagnetism. Other axial-vector currents can be defined which do not have simple anomalous divergence behavior, but these currents are not good prototypes for the physical current.

ACKNOWLEDGMENTS

We wish to thank N. Christ, R. F. Dashen, M. L. Goldberger, and S. B. Treiman for helpful conversations, and R. Jackiw and K. Johnson for a stimulating controversy which led to the writing of this paper. One of us (W.A.B.) wishes to thank Dr. Carl Kaysen for the hospitality of the Institute for Advanced Study.

APPENDIX A

In the first part of this Appendix, we give explicit renormalized expressions for the diagrams depicted in Figs. 12(a) and 12(b), and we show that they satisfy the usual axial-vector Ward identities. In the second part, we demonstrate that the axial-vector–photon–photon–meson box diagram of Fig. 12(f) satisfies the usual axial-vector Ward identity.[19]

A. Meson and Axial-Vector-Current–Meson Loops

In order to give unambiguous values to the divergent loops which we encounter, we define the symmetric, cutoff integral symbol

$$\int_{[C,M^2]} . \tag{A1}$$

Equation (A1) is a shorthand for the following sequence of operations: (i) We do the usual Dyson rotation to the Euclidean region; (ii) we integrate symmetrically over the angle variables around the center $r=C$; and (iii) we integrate the Euclidean magnitude squared $x=-r^2$ up to an upper limit of M^2. Using this symbol, we define *unrenormalized* meson and axial-vector-current–meson loops as follows[20]:

Meson Loops

$$T_\sigma=-G_0\int_{[0,M^2]}\frac{d^4r}{(2\pi)^4}\,\mathrm{Tr}\left(\frac{1}{r-m_0}\right),$$

$$T_{\sigma\sigma}(k)=-i\Sigma_\sigma(k),\quad T_{\pi\pi}(k)=-i\Sigma_\pi(k),$$

$$\Sigma_\sigma(k)=-iG_0^2\int_{[0,M^2]}\frac{d^4r}{(2\pi)^4}\,\mathrm{Tr}\left(\frac{1}{r-m_0}\frac{1}{r-k-m_0}\right),$$

$$\Sigma_\pi(k)=iG_0^2\int_{[0,M^2]}\frac{d^4r}{(2\pi)^4}\,\mathrm{Tr}\left(\gamma_5\frac{1}{r-m_0}\gamma_5\frac{1}{r-k-m_0}\right),$$

[18] Preparata and Weisberger (Ref. 9), Appendix C.

[19] For a derivation of the Ward identities satisfied by the general spinor loop coupling to scalar, pseudoscalar, vector, and axial-vector external sources, with full SU_3 structure, see W. Bardeen (to be published). The results of Appendix A are a special case of the general problem discussed by Bardeen.

[20] In this Appendix, $\Sigma_\pi(k)$ and $\Sigma_\sigma(k)$ denote, respectively, the pion and σ proper self-energies, which were denoted by $\Sigma^\pi(k^2)$ and $\Sigma^\sigma(k^2)$ in the text.

$$T_{\pi\pi\sigma}(k_1,k_2)=2G_0^3\int_{[0,M^2]}\frac{d^4r}{(2\pi)^4}\mathrm{Tr}\left(\gamma_5\frac{1}{r-k_1-m_0}\gamma_5\frac{1}{r+k_2-m_0}\frac{1}{r-m_0}\right),$$

$$T_{\sigma\sigma\sigma}(k_1,k_2)=-2G_0^3\int_{[0,M^2]}\frac{d^4r}{(2\pi)^4}\mathrm{Tr}\left(\frac{1}{r-k_1-m_0}\frac{1}{r+k_2-m_0}\frac{1}{r-m_0}\right),$$

$$T_{\pi\pi\pi\pi}(k_1,k_2,k_3)=-G_0^4\int_{[0,M^2]}\frac{d^4r}{(2\pi)^4}\mathrm{Tr}\left(\gamma_5\frac{1}{r+k_1+k_2+k_3-m_0}\gamma_5\frac{1}{r+k_1+k_2-m_0}\times\gamma_5\frac{1}{r+k_1-m_0}\gamma_5\frac{1}{r-m_0}+\text{five permutations}\right),$$

$$T_{\sigma\sigma\sigma\sigma}(k_1,k_2,k_3)=-G_0^4\int_{[0,M^2]}\frac{d^4r}{(2\pi)^4}\mathrm{Tr}\left(\frac{1}{r+k_1+k_2+k_3-m_0}\frac{1}{r+k_1+k_2-m_0}\times\frac{1}{r+k_1-m_0}\frac{1}{r-m_0}+\text{five permutations}\right),$$

$$T_{\pi\pi\sigma\sigma}(k_1,k_2,k_3)=G_0^4\int_{[0,M^2]}\frac{d^4r}{(2\pi)^4}\mathrm{Tr}\left(\gamma_5\frac{1}{r+k_1+k_2+k_3-m_0}\gamma_5\frac{1}{r+k_1+k_2-m_0}\times\frac{1}{r+k_1-m_0}\frac{1}{r-m_0}+\text{five permutations}\right). \quad \text{(A2)}$$

Axial-Vector-Current–Meson Loops

$$A_\mu(k)=-G_0\int_{[0,M^2]}\frac{d^4r}{(2\pi)^4}\mathrm{Tr}\left(\tfrac{1}{2}\gamma_\mu\gamma_5\frac{1}{r-m_0}\gamma_5\frac{1}{r-k-m_0}\right)+\frac{iG_0m_0}{(4\pi)^2}k_\mu$$

$$=-G_0\int_{[0,M^2e^{1/2}]}\frac{d^4r}{(2\pi)^4}\mathrm{Tr}\left(\tfrac{1}{2}\gamma_\mu\gamma_5\frac{1}{r-m_0}\gamma_5\frac{1}{r-k-m_0}\right), \quad \text{(A3)}$$

$$B_\mu(k_1,k_2)=2G_0^2\int_{[0,M^2]}\frac{d^4r}{(2\pi)^4}\mathrm{Tr}\left(\gamma_5\frac{1}{r-k_1-m_0}\tfrac{1}{2}\gamma_\mu\gamma_5\frac{1}{r+k_2-m_0}\frac{1}{r-m_0}\right).$$

The loops T_σ, $T_{\sigma\sigma}$, $T_{\pi\pi}$, A_μ, and B_μ *are* at least linearly divergent, and so specification of the center for symmetric averaging is essential. The three-meson and four-meson loops, on the other hand, are not linearly divergent, and so the origin of integration in these loops may be freely translated. (Terms which vanish as $M\to\infty$ will be picked up from the translation, but may be ignored. Similarly, the two different expressions which we have given for A_μ are not precisely equal, but differ by terms which vanish as $M\to\infty$.)

We have chosen identical upper limits M^2 for all loop integrals except A_μ, where the upper limit has been taken as $M^2e^{1/2}$ (e is the base of natural logarithms). These choices of upper limit guarantee that the unrenormalized loops satisfy the usual axial-vector Ward identities. For example, in the case of A_μ, a straightforward calculation shows that

$$k^\mu(-G_0)\int_{[0,M^2]}\frac{d^4r}{(2\pi)^4}\mathrm{Tr}\left(\tfrac{1}{2}\gamma_\mu\gamma_5\frac{1}{r-m_0}\gamma_5\frac{1}{r-k-m_0}\right)$$

$$=-\frac{m_0}{G_0}i[\Sigma_\pi(k)-\Sigma_\pi(0)]+\tfrac{1}{2}G_0I(k), \quad \text{(A4)}$$

with

$$I(k)=\int_{[0,M^2]}\frac{d^4r}{(2\pi)^4}\mathrm{Tr}\left(\frac{1}{r-k-m_0}-\frac{1}{r-m_0}\right)$$

$$=\int_{[0,M^2]}\frac{d^4r}{(2\pi)^4}\mathrm{Tr}\left(\frac{1}{r-k-m_0}\not{k}\frac{1}{r-m_0}\not{k}\frac{1}{r-m_0}\right)$$

$$=\frac{-2im_0k^2}{(4\pi)^2}+O(M^{-2}). \quad \text{(A5)}$$

Therefore, $A_\mu(k)$, as defined in Eq. (A3), satisfies the usual axial-vector Ward identity

$$k^\mu A_\mu(k) = -(m_0/G_0)i[\Sigma_\pi(k)-\Sigma_\pi(0)]. \quad \text{(A6)}$$

Similarly, the axial-vector triangle $B_\mu(k_1,k_2)$ satisfies the Ward identity

$$-(k_1+k_2)^\mu B_\mu(k_1,k_2) = (m_0/G_0)T_{\pi\pi\sigma} + i\Sigma_\sigma(k_2) - i\Sigma_\pi(k_1). \quad \text{(A7)}$$

The axial-vector-current–three-meson box diagram of Fig. 12(b) is superficially logarithmically divergent, but, because $\mathrm{Tr}\{\gamma_\mu\gamma_5 r(1,\gamma_5)r(1,\gamma_5)r(1,\gamma_5)r\}=0$, this diagram actually converges, which is why we have not included it in the list of unrenormalized axial-vector-current loops in Eq. (A3). Introducing a cutoff at $x=M^2$ (which changes this diagram only by terms which vanish as $M\to\infty$) and then taking the divergence yields a linear combination of three- and four-meson loop diagrams, all with cutoff at $x=M^2$ as in Eq. (A2) Some of these loops may occur with the loop integration variable translated by a finite amount with respect to the standard forms in Eq. (A2), but as we have pointed out, this does not matter because none of the three- or four-meson loops is linearly divergent. We conclude, then, that the axial-vector-current–three-meson box diagram and the meson loop diagrams of Eq. (A2) satisfy the usual axial-vector Ward identity. Identical reasoning shows that the axial-vector-current–four-meson pentagon, which is superficially convergent, is related by the usual Ward identity to a linear combination of the meson box diagrams of Eq. (A2) and to the convergent meson pentagon diagram. Note that because the axial-vector-current box and pentagon diagrams are *finite*, their Ward identities will necessarily involve linear combinations of the meson triangle and box diagrams in which the logarithmic divergences exactly cancel.

Having defined the unrenormalized loop diagrams and shown that they satisfy the correct Ward identities, we next construct the renormalized loops and show that they, too, satisfy the proper Ward identities. The renormalized meson scattering and axial-vector-current loops are obtained from the unrenormalized loops by adding appropriate matrix elements of $i\mathfrak{L}^{\text{counter}}$ and $j_\mu{}^{5\ \text{counter}}$ with [see Eqs. (57) and (59)]

$$\mathfrak{L}^{\text{counter}} = D^{(2)}[4\sigma^2+4(G_0/m_0)\sigma(\sigma^2+\pi^2) + (G_0/m_0^2)(\sigma^2+\pi^2)^2] + \tfrac{1}{2}E^{(2)}[(\partial\pi)^2+(\partial\sigma)^2] + \tfrac{1}{2}F^{(2)}[(2m_0/G_0)\sigma+\sigma^2+\pi^2], \quad \text{(A8)}$$

$$j_\mu{}^{5\ \text{counter}} = E^{(2)}[\sigma\partial_\mu\pi - \pi\partial_\mu\sigma + (m_0/G_0)\partial_\mu\pi].$$

The subtractions $D^{(2)}$, $E^{(2)}$, and $F^{(2)}$ are determined from the second-order π and σ self-energy diagrams to be

$$D^{(2)} = \frac{m_0^2G_0^2}{(4\pi)^2}\ln\left(\frac{M^2}{m_0^2}\right)+\bar{D}^{(2)},$$
$$E^{(2)} = \frac{-2G_0^2}{(4\pi)^2}\ln\left(\frac{M^2}{m_0^2}\right)+\bar{E}^{(2)},$$
$$F^{(2)} = \Sigma_\pi(0) = iG_0^2\int_{[0,M^2]}\frac{d^4r}{(2\pi)^4} \times \mathrm{Tr}\left(\gamma_5\frac{1}{r-m_0}\gamma_5\frac{1}{r-m_0}\right). \quad \text{(A9)}$$

The finite constants $\bar{D}^{(2)}$ and $\bar{E}^{(2)}$ are adjusted to give the physical pion mass and the meson-meson scattering constant the specified values μ^2 and λ. The renormalized loops, denoted by a tilde, are given by

$$\begin{aligned}
\tilde{T}_\sigma &= T_\sigma + i(m_0/G_0)F^{(2)} = 0,\\
\tilde{\Sigma}_\pi(k) &= \Sigma_\pi(k) - F^{(2)} - k^2E^{(2)},\\
\tilde{\Sigma}_\sigma(k) &= \Sigma_\sigma(k) - F^{(2)} - 8D^{(2)} - k^2E^{(2)},\\
\tilde{T}_{\pi\pi\sigma} &= T_{\pi\pi\sigma} + 8i(G_0/m_0)D^{(2)},\\
\tilde{T}_{\sigma\sigma\sigma} &= T_{\sigma\sigma\sigma} + 24i(G_0/m_0)D^{(2)},\\
\tilde{T}_{\pi\pi\pi\pi} &= T_{\pi\pi\pi\pi} + 24i(G_0^2/m_0^2)D^{(2)},\\
\tilde{T}_{\sigma\sigma\sigma\sigma} &= T_{\sigma\sigma\sigma\sigma} + 24i(G_0^2/m_0^2)D^{(2)},\\
\tilde{T}_{\pi\pi\sigma\sigma} &= T_{\pi\pi\sigma\sigma} + 8i(G_0^2/m_0^2)D^{(2)},\\
\tilde{A}_\mu(k) &= A_\mu(k) + i(m_0/G_0)E^{(2)}k_\mu,\\
\tilde{B}_\mu(k_1,k_2) &= B_\mu(k_1,k_2) + iE^{(2)}(k_2-k_1)_\mu.
\end{aligned} \quad \text{(A10)}$$

It is straightforward to verify that all of the tilde quantities approach finite limits as $M\to\infty$, showing, as required by chiral invariance, that the subtraction constants determined from the second-order loops make the triangle and box diagrams finite as well.

From Eqs. (A6), (A7), and (A10) we find that the renormalized loops $\tilde{A}_\mu$ and $\tilde{B}_\mu$ satisfy the desired Ward identities

$$\begin{aligned}
k^\mu\tilde{A}_\mu(k) &= -i(m_0/G_0)\tilde{\Sigma}_\pi(k),\\
-(k_1+k_2)^\mu\tilde{B}_\mu(k_1,k_2) &= (m_0/G_0)\tilde{T}_{\pi\pi\sigma} + i\tilde{\Sigma}_\sigma(k_2) - i\tilde{\Sigma}_\pi(k_1).
\end{aligned} \quad \text{(A11)}$$

Next, we recall that the axial-vector-current box and pentagon diagrams and the unrenormalized meson-scattering triangle and box diagrams are related by the usual Ward identities. This implies that the same Ward identities are satisfied by the axial-vector box and pentagon and the *renormalized* meson-scattering diagrams. The reason is that the counter terms which subtract the divergences in the meson loops necessarily occur in each Ward identity in the same linear combination as the logarithmic divergences, and therefore cancel among themselves in the Ward identity in the same manner as the logarithmic divergences do. This com-

pletes the proof that the renormalized basic loop diagrams satisfy the normal axial-vector Ward identities.

B. Axial-Vector-Current–Photon–Photon–Meson Loop [Figure 12(f)]

The Ward identity for the axial-vector-current–photon–photon–meson loop of Fig. 12(f) relates it to a linear combination of the diagrams shown in Fig. 12(e), plus a possible anomalous term. To see that no anomalous term is actually present, we note that: (i) Gauge invariance makes the diagrams of Figs. 12(e) and 12(f) finite, so no renormalizations are needed to make the various terms in the Ward identity well defined; (ii) a possible anomalous term must be gauge-invariant with respect to both photon indices, must be odd in m_0, and must have the dimensions of a mass, since all of the other terms in the Ward identity have these properties; (iii) a possible anomalous term can have *no singularities* in internal masses or external momentum variables, since taking an absorptive part eliminates the superficially logarithmically or linearly divergent loop integrals, and therefore the absorptive parts satisfy the usual Ward identities. According to (ii), a possible anomalous term must have the form

$$\text{anomalous term} \propto m_0 F_1 F_2 / g(m_0, \text{external momenta}), \quad \text{(A12)}$$

where F_1 and F_2 are the two photon field strength tensors and where g has the dimensions of (mass)^2. However, because of the division by g, Eq. (A12) necessarily has singularities, and therefore (iii) forces the anomalous term to be zero.

APPENDIX B

We state here the renormalized second-order vector vertex, pseudoscalar vertex, and fermion propagator used in the calculation of Sec. III.

$$\tilde{\Gamma}_\lambda^{(2)}(p,p')=\gamma_\lambda+\frac{c^2}{16\pi^2}\int_0^1 zdz\int_0^1 dy\left\{2\gamma_\lambda\ln\left[\frac{z^2m^2+(1-z)\mu^2}{D}\right]-\frac{N_\lambda}{D}-\frac{2m^2\gamma_\lambda P_1}{z^2m^2+(1-z)\mu^2}\right\},$$

$$\tilde{\Gamma}_5^{(2)}(p,p')=\gamma_5+\frac{c^2}{16\pi^2}\int_0^1 zdz\int_0^1 dy\left\{8\gamma_5 f\ln\left[\frac{z^2m^2+(1-z)\mu^2}{D}\right]+\frac{\gamma_5 N}{D}+\frac{4m^2\gamma_5 P_2}{z^2m^2+(1-z)\mu^2}\right\},$$

$$\tilde{S}_F'^{(2)}(p)=[\not p-m-\Sigma(\not p)]^{-1}, \quad \text{(B1)}$$

$$\Sigma(\not p)=\frac{c^2}{16\pi^2}\int_0^1 zdz\left\{2g_1\ln\left[\frac{z^2m^2+(1-z)\mu^2}{-p^2z(1-z)+zm^2+(1-z)\mu^2}\right]+g_2\frac{m^2-p^2(1-z)^2}{-p^2z(1-z)+zm^2+(1-z)\mu^2}+\frac{2m^2\not pP_1+4m^3P_2}{z^2m^2+(1-z)\mu^2}\right\},$$

$$D=(y^2z^2-yz)p^2+[(1-y)^2z^2-(1-y)z]p'^2+2y(1-y)z^2p\cdot p'+zm^2+(1-z)\mu^2.$$

The quantities c, N_λ, N, P_1, P_2, f, g_1, and g_2 are defined as follows:

Spinor Electrodynamics

$$c=e,$$

$$N_\lambda=-2m^2\gamma_\lambda-2[(1-z+yz)\not p'-yz\not p]\times\gamma_\lambda[(1-yz)\not p-(1-y)z\not p']+4m[(1-2yz)p_\lambda+(1-2z+2yz)p_\lambda'],$$

$$N=4m^2-4[(1-yz)p-(1-y)zp']\cdot\times[(1-z+yz)p'-yzp]+2m(\not p-\not p'), \quad \text{(B2)}$$

$$P_1=z^2+2z-2,\quad P_2=1-2z,$$

$$f=1,$$

$$g_1=4m-\not p,\quad g_2=4m-2\not p.$$

σ Model

$$c=G,$$

$$N_\lambda=-2m^2\gamma_\lambda-2[(1-yz)\not p-(1-y)z\not p']\times\gamma_\lambda[(1-z+yz)\not p'-yz\not p],$$

$$N=-2m(\not p-\not p'), \quad \text{(B3)}$$

$$P_1=z^2-2z+2,\quad P_2=-(1-z)^2,$$

$$f=0,$$

$$g_1=-\not p,\quad g_2=-2\not p.$$

APPENDIX C

We show that the integral

$$I(a)\equiv\int_0^1 zdz\int_0^\infty\frac{udu}{(u+1)^3}\frac{1-u(1-z)}{uz(1-z)+z+(1-z)a} \quad \text{(C1)}$$

is identically zero. We begin by observing that $I(a)$ is analytic in the a plane, apart from a cut along the real axis from 0 to $-\infty$. The discontinuity across this cut at $a=-A$ is proportional to

$$\rho(A)\equiv\int_0^1\frac{zdz}{1-z}\int_0^\infty\frac{udu}{(u+1)^3}\times[1-u(1-z)]\delta(uz+z/(1-z)-A)$$
$$=\int_0^{A/(A+1)}dz\frac{z(1-z)[A-(A+1)z][(2+A)z-A]}{[-z^2+A(1-z)]^3}$$
$$=-\frac{1}{2A}\int_0^{A/(A+1)}dz\frac{d}{dz}\left\{\frac{z^2[A-(A+1)z]^2}{[-z^2+A(1-z)]^2}\right\}=0, \quad \text{(C2)}$$

which means that $I(a)$ is an entire function. Furthermore, for $\mathrm{Re}a\geq 0$,

$$|I(a)|\leq\int_0^1 dz\int_0^\infty\frac{udu}{(u+1)^3}\left|\frac{z+uz(1-z)}{uz(1-z)+z+(1-z)a}\right|$$
$$\leq\int_0^1 dz\int_0^\infty\frac{udu}{(u+1)^3}=\frac{1}{2} \quad \text{(C3)}$$

and

$$I(0)=2\int_0^\infty\frac{udu}{(u+1)^3}\int_0^1\frac{dz}{u(1-z)+1}-\int_0^\infty\frac{udu}{(u+1)^3}=\frac{1}{2}-\frac{1}{2}=0. \quad \text{(C4)}$$

Since Feynman integrals like Eq. (C1) never lead to functions of exponential type, Eqs. (C1)–(C4) show that $I(a)\equiv 0$.

PHYSICAL REVIEW VOLUME 182, NUMBER 5 25 JUNE 1969

Deck Effect with K Exchange*

KWAN WU LAI
Physics Department, Brookhaven National Laboratory, Upton, New York 11973

AND

JOSEPH M. SHPIZ
The City College of the City University of New York, New York, New York 10031
Brookhaven National Laboratory, Upton, New York 11973

(Received 27 January 1969)

It is shown that the nature of the vertex function for $\bar{K}N\to\Lambda\pi$ favors a kinematical configuration of the $\rho\pi\Lambda$ in $\bar{K}N\to\Lambda\pi\rho$ which effectively competes with the kinematical configuration responsible for the Deck effect, and substantially flattens the low-mass enhancement. This reaction is thus a far more suitable one in which to verify and study the A_1 $(\rho\pi)$ enhancement. These results should also be applicable to a study of the $K^*(1300)$ in the reaction $\pi N\to\Lambda K^*(890)\pi$.

A MAJOR difficulty in the experimental analysis of low-mass enhancements such as the $A_1(1080)$ in the reaction[1] $\pi N\to\rho\pi N$ and the $K^*(1300)$ in the reaction $KN\to K^*(890)\pi N$ is the possible presence of strong kinematic background, from the Deck-type mechanism, centered about the low-mass region of interest. Intrinsic ambiguities in the calculations of these kinematic effects have further prevented a firm experimental answer to the question of the existence of these low-mass resonances. In this paper we examine the conjecture[2] that the Deck-type mechanism plays a substantially weaker role in the reactions $\bar{K}N\to\Lambda\rho\pi$ and $\pi\rho\to\Lambda K^*(890)\pi$. Our analysis provides strong support for the correctness of this conjecture, and hence these reactions are more suitable for studies of low-mass resonances such as the A_1 and the $K^*(1300)$.

In Fig. 1 particles 3 and 5 are baryons and particle 1 is either a K or π, while particle 4 is a vector particle, $\rho(760)$ or $K^*(890)$. The original calculation[3] by Deck computed the 3+4 mass spectrum assuming that the virtual scattering $2+3\to 5+6$ (πN elastic scattering) is sharply peaked forward and essentially constant in energy. The result of this calculation is that the 4+5 mass distribution is greatly enhanced at low mass values, corresponding to the sometimes observed A_1. Stodolsky[4] has presented an explanation of this enhancement based on the observation that the $\Delta^2+m_2^2$ denominator, together with the diffraction nature of

* Work performed at Brookhaven National Laboratory was under the auspices of the U. S. Atomic Energy Commission. Work performed at City College was supported in part by a City University Summer Research Grant.

[1] The A_1 was first reported by Bellini *et al.*, Nuovo Cimento **29**, 896 (1963). Additional references may be found in Particle Data Group, Rev. Mod. Phys. **41**, 109 (1969).

[2] D. J. Crennell, G. R. Kalbfleisch, K. W. Lai, J. M. Scarr, and T. G. Schumann, Phys. Rev. Letters **19**, 44 (1967).

[3] R. T. Deck, Phys. Rev. Letters **13**, 169 (1964); U. Maor and T. A. O'Halloran, Jr., Phys. Letters **15**, 281 (1965). For a more recent analysis see M. Ross and Y. Yam, Phys. Rev. Letters **19**, 546 (1967); for an alternative explanation of the A_1, see N. P. Chang, *ibid.* **14**, 806 (1965).

[4] L. Stodolsky, Phys. Rev. Letters **18**, 973 (1967).